Publicaciones Geológicas Especiales

SERVICIO GEOLÓGICO COLOMBIANO

El futuro es de todos | Minenergía

ISBN: 978-958-52959-2-6

The Geology of Colombia book provides an updated background of the geological knowledge of Colombia by integrating the most up–to–date research covering paleontology, biostratigraphy, sedimentary basin analysis, sedimentology, sequence stratigraphy, stratigraphy, geophysics, geochronology, geochemistry, thermochronology, tectonics, structure, volcanology, petrology, environmental science, climate change, and space geodesy.

Each chapter has a complete framework of a major branch of geology providing an invaluable resource for geologists interested in the geological history of Colombia.

The first volume presents a comprehensive, ten chapter overview covering the physiographic and geological setting in Colombia, geophysical data of eastern Colombia, continental tectonostratigraphic terranes in Colombia, evolution of the Proterozoic basement of the West Guyana Shield, the Putumayo Orogen of Amazonia, the Ediacaran and Paleozoic in the Llanos Basin and Colombian Andes, and the Permian arc on the western margin of the Neoproterozoic basement of Colombia.

Other volumes in *The Geology of Colombia* book
Volume 2: Mesozoic
Volume 3: Paleogene – Neogene
Volume 4: Quaternary

Jorge GÓMEZ TAPIAS
Daniela MATEUS–ZABALA
Editors

THE GEOLOGY OF COLOMBIA
VOLUME 1 • PROTEROZOIC – PALEOZOIC

35

THE GEOLOGY OF COLOMBIA

VOLUME 1 • PROTEROZOIC – PALEOZOIC

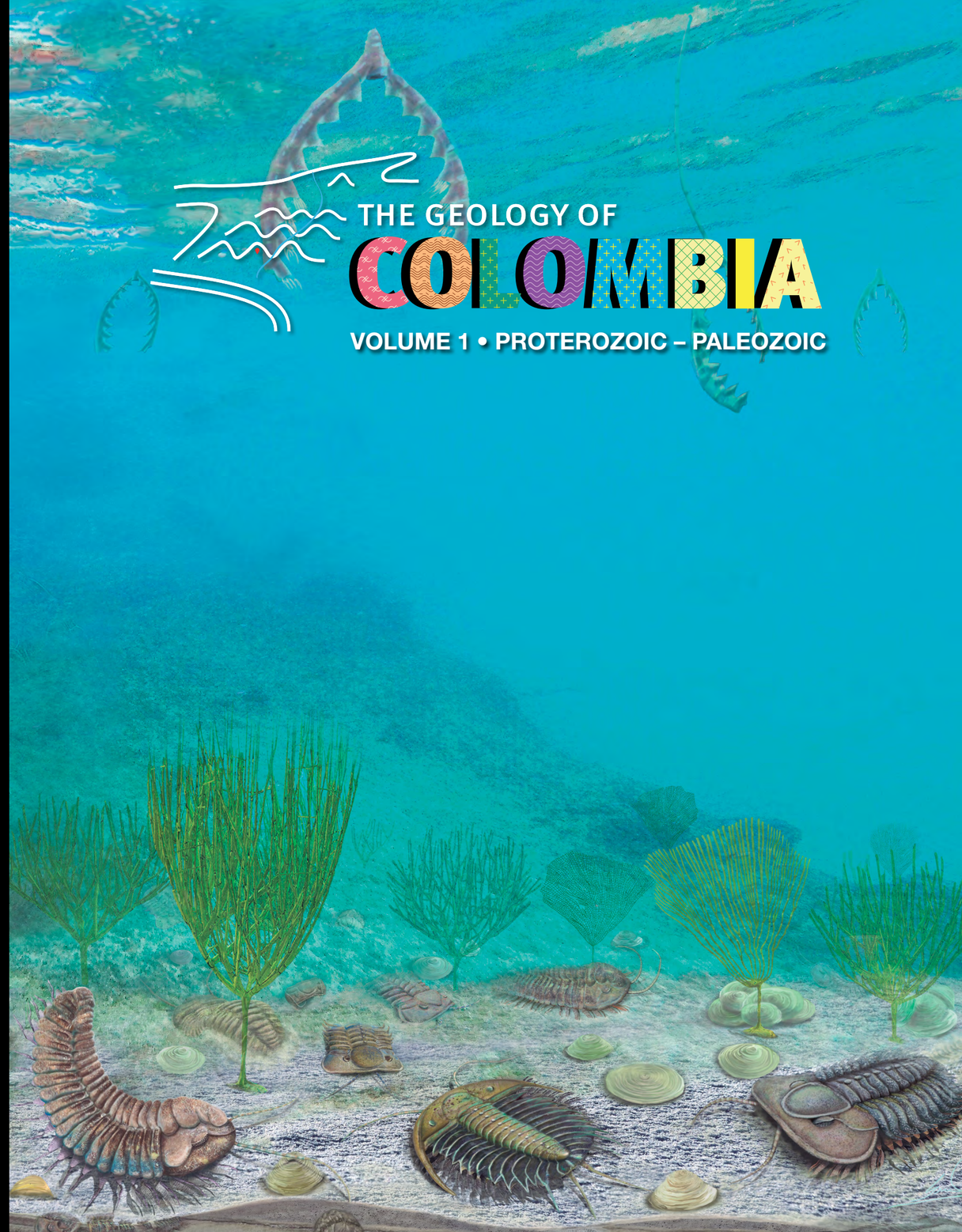

Volume 1

Chapter 4

https://doi.org/10.32685/pub.esp.35.2019.04
Published online 24 November 2020

Zircon U–Pb Geochronology and Hf–Nd–O Isotope Geochemistry of the Paleo– to Mesoproterozoic Basement in the Westernmost Guiana Shield

Mauricio IBAÑEZ–MEJIA[1]* and Umberto G. CORDANI[2]

1 ibanezm@arizona.edu
Department of Geosciences
University of Arizona
Tucson, Arizona, 85721, USA

2 ucordani@usp.br
Universidade de São Paulo
Instituto de Geociências
São Paulo–SP, Brasil

* Corresponding author

Abstract The crystalline basement of eastern Colombia, east of the frontal deformation zone of the north Andean Eastern Cordillera, is comprised by Precambrian igneous, metamorphic, and sedimentary rocks of the western Guiana Shield. Designated in the late seventies with the all–embracing stratigraphic name of 'Mitú Migmatitic Complex', the age, petrology, and tectonic history of the Precambrian basement in eastern Colombia has remained one of the least explored issues in South American geology. This chapter aims to present a brief overview of recent advances made to improve our general understanding of the geology of this wide region, using a compilation of the available U–Pb, Sm–Nd, Lu–Hf, and $\delta^{18}O$ isotopic data obtained using modern methods. Using all the available U–Pb geochronologic data we show that, in general: (i) The Precambrian basement of the western Guiana Shield exhibits magmatic crystallization ages in the range from ca. 1.99 to ca. 1.38 Ga, and (ii) that four broad periods of magmatic activity, two in the mid– to late–Paleoproterozoic (ca. 1.99 and ca. 1.81–1.72 Ga), one in the early Mesoproterozoic (ca. 1.59–1.50 Ga), and one in the mid Mesoproterozoic (ca. 1.41–1.39 Ga) dominate the geology of the area. The (whole–rock) Nd and combined (zircon) Hf–O datasets indicate a general lack of 'depleted mantle' like mid–Paleoproterozoic or Mesoproterozoic crust, thus indicating that either the Proterozoic sub–continental mantle in the region was not as radiogenic as global mantle evolution models would suggest, or that reworking of older crust might have played an important role in the geological and geochemical evolution of the western Guiana Shield. Therefore, although the geochronologic results confirm that most of the exposed basement in eastern Colombia can be broadly considered to be of Rio Negro–Juruena–like affinity, this belt exhibits some distinct isotopic characteristics relative to similar age domains exposed south of the Amazon Basin. Furthermore, we note that the geochronologic data obtained to this date has failed to clearly identify an early– to mid–Mesoproterozoic terrane boundary in the Colombian basement, thus opening the possibility that a Rondonian–San Ignacio–like province is not represented in the Guiana Shield. Based on these recent field, geochemical, and geochronological observations, we consider the long and extensively used term 'Mitú Migmatitic Complex' to be now inadequate and obsolete, and argue that the current state of the knowledge of the Colombian Precambrian basement is such that the community should move towards adopting

Citation: Ibañez–Mejia, M. & Cordani, U.G. 2020. Zircon U–Pb geochronology and Hf–Nd–O isotope geochemistry of the Paleo– to Mesoproterozoic basement in the westernmost Guiana Shield. In: Gómez, J. & Mateus–Zabala, D. (editors), The Geology of Colombia, Volume 1 Proterozoic – Paleozoic. Servicio Geológico Colombiano, Publicaciones Geológicas Especiales 35, p. 65–90. Bogotá. https://doi.org/10.32685/pub.esp.35.2019.04

more accurate and modern petrologic, tectonic, and stratigraphic nomenclature. Lastly, we note that the recent discovery of Cretaceous magmatism affecting the Colombian continental interior in the Araracuara basement high highlights the importance of Mesozoic tectonic reactivation in controlling the structural and landscape evolution of the Colombian Amazon. This observation indicates that future geochronologic studies aimed at better understanding the temporal history of mafic magmatism in this region will be crucial for understanding its structural and tectonic evolution.
Keywords: *Amazonian Craton, Proterozoic tectonics, U–Pb geochronology, Lu–Hf isotopes, Sm–Nd isotopes.*

Resumen El basamento cristalino del oriente colombiano, al este del frente de deformación andino de la cordillera Oriental, está compuesto por rocas ígneas, metamórficas y sedimentarias precámbricas pertenecientes al Escudo de Guayana. Agrupadas en la década de los setenta dentro de una unidad estratigráfica conocida como 'Complejo Migmatítico de Mitú', la edad, petrología, e historia tectónica de las unidades del basamento precámbrico en el oriente colombiano han permanecido como uno de los problemas menos explorados de la geología suramericana. Este capítulo tiene como objetivo presentar una revisión breve sobre los avances hechos en los últimos años para mejorar nuestro entendimiento geológico de esta amplia región, a partir de una compilación de información isotópica obtenida usando los sistemas U–Pb, Sm–Nd, Lu–Hf y $\delta^{18}O$ con métodos analíticos modernos. Considerando los datos de geocronología U–Pb disponibles observamos que en general: (1) el basamento precámbrico del límite occidental del Escudo de Guayana exhibe edades de cristalización en el rango de ca. 1,99 a ca. 1,38 Ga y (2) que cuatro principales eventos de actividad magmática, dos en el Paleoproterozoico medio a tardío (ca. 1,99 y ca. 1,81–1,72 Ga), uno en el Mesoproterozoico temprano (ca. 1,59–1,50 Ga) y uno en el Mesoproterozoico medio (ca. 1,41–1,39 Ga), dominan la geología de esta región. Las composiciones isotópicas de Nd en roca total junto con resultados conjuntos de isótopos de Hf y O en circón indican una ausencia generalizada de material directamente derivado del 'manto empobrecido' en este basamento paleo– y mesoproterozoico. Dicha observación puede deberse a dos motivos particulares: (1) que el manto sublitosférico proterozoico en la región no era tan radiogénico como la mayoría de los modelos globales de evolución mantélica sugerirían o (2) que el retrabajamiento de corteza continental más antigua podría haber jugado un papel importante en la evolución geológica y geoquímica del occidente del Escudo de Guayana. Por consiguiente, a pesar de que los resultados geocronológicos confirman que la mayor parte del basamento expuesto en el oriente colombiano puede considerarse a grandes rasgos como afín a la Provincia Río Negro–Juruena, la margen occidental del Escudo de Guayana presenta características isotópicas distintivas con respecto a los dominios de basamento de edad semejante expuestos al sur de la Cuenca del Amazonas. En adición a lo antedicho, observamos que la base de datos geocronológica existente no permite a la fecha identificar claramente una sutura mesoproterozoica temprana a media en el basamento del oriente colombiano, lo que sugiere la posibilidad de que un dominio de basamento afín a la Provincia Rondoniana–San Ignacio no este expresado en el Escudo de Guayana. Basados en las observaciones de campo, geoquímicas y geocronológicas presentadas en este capítulo consideramos que el término estratigráfico 'Complejo Migmatítico de Mitú', que ha sido ampliamente usado, resulta ahora inadecuado para describir la complejidad geológica del área y por consiguiente es obsoleto. En lugar de esto, consideramos que el estado del conocimiento geológico del oriente colombiano ha avanzado lo suficiente para permitir que una nomenclatura petrológica, tectónica y estratigráfica moderna, que describa con mayor exactitud la geología del área y por ende más apropiada, sea adoptada. Para

concluir, también observamos que el descubrimiento reciente de magmatismo de edad cretácica que afecta el interior continental colombiano en el alto de basamento de Araracuara resalta la importancia que la reactivación tectónica mesozoica tuvo en el desarrollo estructural y geomorfológico de la Amazonia colombiana. Esta observación indica que los futuros estudios geocronológicos enfocados a comprender mejor la historia temporal del magmatismo máfico en esta región serán cruciales para mejorar nuestro entendimiento sobre la evolución estructural y tectónica del oriente colombiano.

Palabras clave: *Cratón Amazónico, tectónica proterozoica, geocronología U–Pb, geoquímica isotópica Lu–Hf, geoquímica isotópica Sm–Nd.*

1. Introduction

The continental basement of eastern Colombia, stretching from the Andean deformation front in the Llanos foothills to the borders with Venezuela and Brasil in the Orinoco and Amazonas territories, is comprised by Precambrian rocks of the western Guiana Shield (Figure 1; Cordani et al., 2016a; Gómez et al., 2017). Although most of the crystalline basement east of the Andes is currently buried under the thick sedimentary cover of the Putumayo and Llanos Foreland Basins, exposures of Precambrian igneous and metamorphic rocks occur in theVichada, Guainía, Vaupés, Caquetá, and Guaviare Departments (Figure 2). Difficulty of access to these areas, however, combined with the lack of roads and widespread vegetation cover, have made the geology of this region to remain relatively unexplored even to this date.

The Precambrian geology of Colombia bears great importance for understanding the growth history and paleogeography of the Amazonian Craton throughout the Proterozoic. The paleocontinent known as *Amazonia* is not only one of the largest Precambrian crustal nuclei on Earth but is also thought to have played a key role in the Precambrian supercontinent cycle (e.g., Cordani et al., 2009). Thus, understanding the construction of the Colombian Precambrian shield, and its potential correlation (or lack thereof) with crustal domains exposed south of the Amazon Basin, is a critical step toward reconstructing the tectonic history and assembly of Amazonia. Furthermore, understanding the geology of the Colombian basement is not only critical for correlating intra–cratonic structures, but also for evaluating potential connections amongst ancient orogenic belts across separate cratonic blocks that may once have been juxtaposed, therefore providing vital information for Precambrian paleogeography and supercontinent reconstructions (e.g., Li et al., 2008). All this information, however, can only be appropriately assessed if an adequate knowledge of the local geology is gained, and this is precisely why geologic, geochronologic, and isotopic studies from the eastern Colombian basement are of fundamental importance.

Over the past few years, a handful of studies have been published providing new geochronologic and isotopic data from the Precambrian basement of the westernmost Guiana Shield. These new results not only allow revisiting some of the paradigms that have prevailed in our understanding of the Colombian geology for many decades, but also to begin developing new ones. In this chapter, we provide a brief synthesis of the current state of knowledge on the geology of the Precambrian basement of the westernmost Guiana Shield, particularly focusing on the geochronologic and isotopic data obtained in Colombian territory over the last decade using modern U–Pb, Lu–Hf, and Sm–Nd methods. For a discussion of other available data using the Rb–Sr and K–Ar isotopic systems, the reader is referred to the recent comprehensive discussion provided by Cordani et al. (2016b).

2. Previous Studies and Geological Background

The first geochronologic analyses from the eastern Colombian basement were conducted by Pinson et al. (1962), where these authors performed K–Ar and Rb–Sr isotopic analyses of biotites from the San José del Guaviare syenites and porphyroblastic granitoids along the Guaviare River. They obtained ages around 1.2 Ga for the granitoids and around 460 Ma for the syenites. However, after this groundbreaking study by Pinson and co–workers, nearly two decades would have to go by before any new geochronologic data was produced.

In the late seventies, the 'Proyecto Radargramétrico del Amazonas' (PRORADAM) took place, and the results from this extensive field reconnaissance, mapping, and petrographic study were published by Galvis et al. (1979). This project also involved Rb–Sr, K–Ar, and the first U–Pb analyses performed in the area, which were conducted by the Z.W.O Isotope Geology Laboratory in Amsterdam and were published by Priem et al. (1982). These authors presented the first U–Pb concordia diagrams for ca. 1.55 Ga granitoids from the Vaupés River, identified ca. 1.8 Ga inherited components in zircons from gneisses in the Guainía River, and presented extensive Rb–Sr results suggesting the occurrence of magmatic events ca. 1.8 Ga, 1.55 Ga throughout the region. They also identified mafic rocks that defined apparent Rb–Sr isochron relations with slopes ca. 1.2 Ga, and a suite of rhyodacitic lavas from the Vaupés River with an apparent isochron age of ca. 920 Ma. This study was certain-

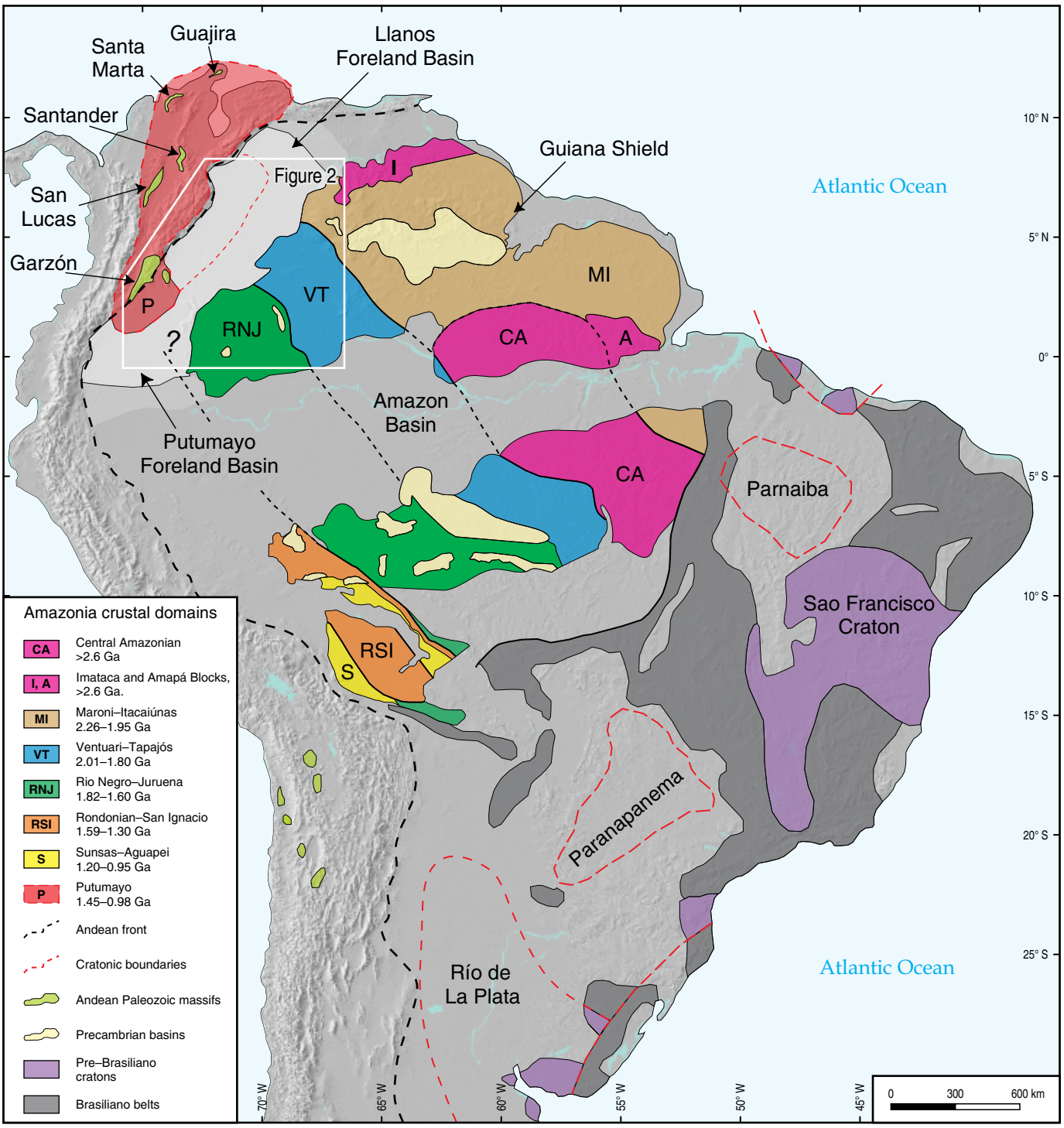

Figure 1. Simplified geo–tectonic map of South America overlaid on gray–scale shaded relief image (DEM), highlighting the approximate outline and terrane boundaries of the Amazonian Craton and the Guiana Shield. Adapted from Cordani & Teixeira (2007), Fuck et al. (2008), Ibañez–Mejia et al. (2015), Tassinari & Macambira (1999), and Teixeira et al. (2019). Shaded relief image areas with no overlay indicate younger cratonic cover or units in the Andean region. Light–gray shaded region indicates the location and extent of the north Andean Putumayo and Llanos Foreland Basins.

ly revolutionary, and set the stage for understanding the geology of eastern Colombia for the following ca. 30 years.

Although not strictly within Colombian territory, other studies conducted in SW Venezuela and NW Brasil in the late seventies and early nineties were also seminal for developing a better understanding of the geology of the western Guiana Shield; these were published by Barrios (1983), Barrios et al. (1985, 1986), Cordani et al. (1979), Fernandes et al. (1976),

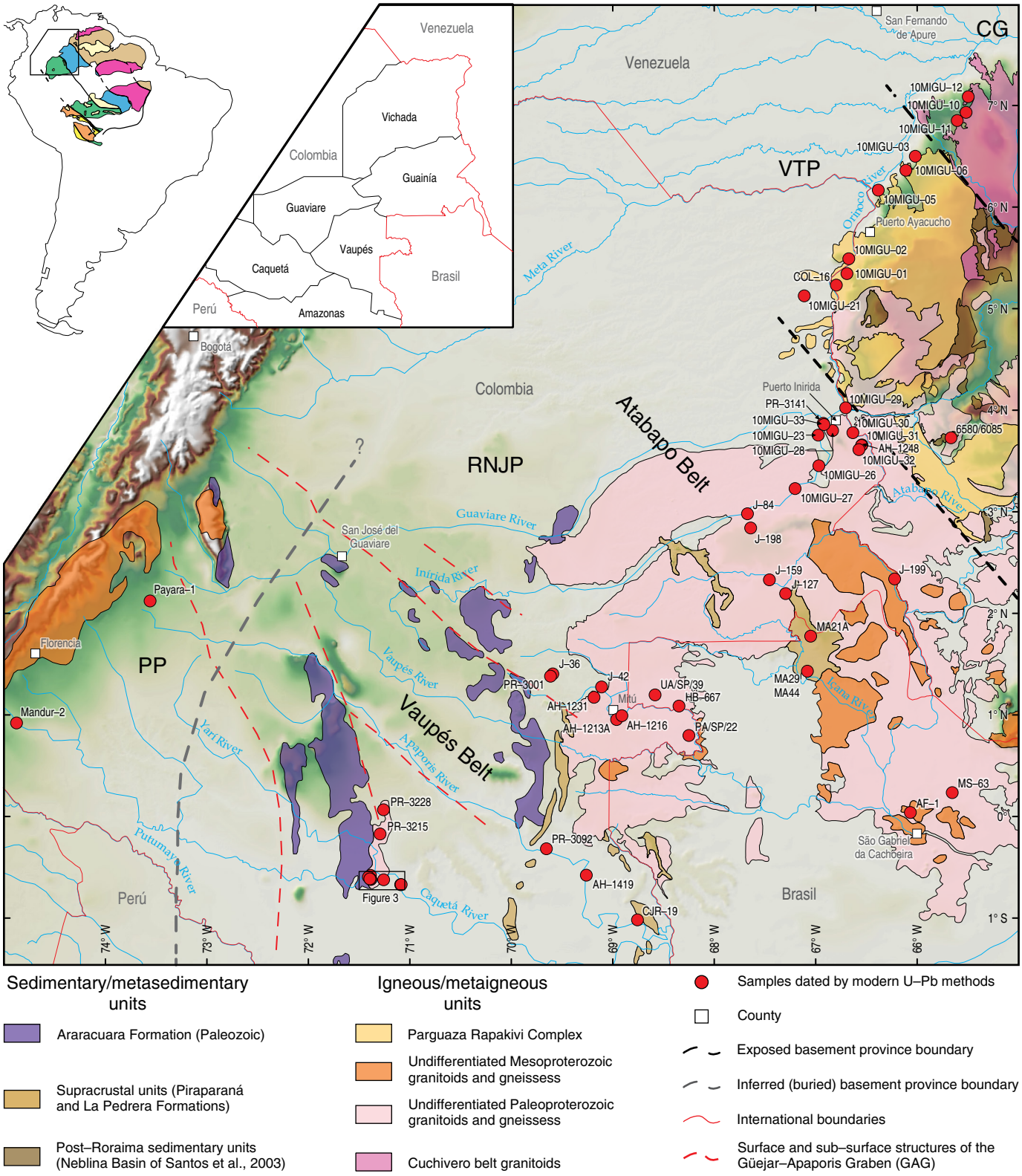

Sedimentary/metasedimentary units

- Araracuara Formation (Paleozoic)
- Supracrustal units (Piraparaná and La Pedrera Formations)
- Post–Roraima sedimentary units (Neblina Basin of Santos et al., 2003)

Igneous/metaigneous units

- Parguaza Rapakivi Complex
- Undifferentiated Mesoproterozoic granitoids and gneissess
- Undifferentiated Paleoproterozoic granitoids and gneissess
- Cuchivero belt granitoids

- Samples dated by modern U–Pb methods
- County
- Exposed basement province boundary
- Inferred (buried) basement province boundary
- International boundaries
- Surface and sub–surface structures of the Güejar–Apaporis Graben (GAG)

Figure 2. Simplified geologic map of the westernmost Guiana Shield, adapted from the maps of Cordani et al. (2016a) and Gómez et al. (2017). Inset shows the location and boundaries of Colombian departments mentioned throughout the text. Black dashed lines are major exposed intra–cratonic boundaries as suggested from the existing geochronologic data, namely: (1) The limit between the felsic volcanics of the Cuchivero Group (CG) in Venezuela, and the southern part of the Ventuari–Tapajós Province (VTP), and (2) the limit between VTP and Rio Negro–Juruena Province (RNJP), drawn along the Atabapo River as suggested by Cordani et al. (2016a). The dashed gray line outlines an approximate location for the suture between the RNJP and the Putumayo Province (PP), whose exact location is currently unknown. Red dashed lines reflect the approximate traces of faults associated with the intra–cratonic Güejar–Apaporis Graben (GAG).

Gaudette & Olszewski (1985), Gaudette et al. (1978), Gibbs & Barron (1993), and Pinheiro et al. (1976). Most of these studies exclusively employed Rb–Sr and K–Ar methods, with the exception of Gaudette & Olszewski (1985) and Gaudette et al. (1978) who presented the first U–Pb geochronologic result of intrusives from the Parguaza intrusive complex and the Minicia and Macabana gneisses along the Orinoco and Ventuari Rivers in Venezuela. Based on upper intercepts of discordia regressions through strongly discordant zircon U–Pb data (from dissolution of multi–grain aliquots), these authors proposed an age of ca. 1.55 Ga for the Parguaza complex and ages around 1.82 and 1.86 Ga for the Macabana and Minicia gneisses, respectively. It is worth noting that these results were obtained using a 12–inch, 60˚sector mass spectrometer at Massachusetts Institute of Technology (MIT; Aldrich et al., 1953; Herzog, 1952; Shrock, 1977), which is in principle the same design that Alfred O. NIER used to separate the isotopes of uranium during World War II (Nier, 1940, 1947). Although the age results obtained using these instruments were certainly remarkable for the time, we consider them as 'legacy' data for the purposes of this discussion and only mention them here because of their particular historical significance.

In 1996, the first SHRIMP U–Pb analyses on zircons from the region were published by Tassinari et al. (1996), marking the beginning of what we here consider as 'modern methods' from a U–Pb geochronology standpoint. As mentioned previously, this chapter will not take into consideration the Rb–Sr and K–Ar databases, because a comprehensive compilation and careful analysis of these results was recently done by Cordani et al. (2016b), and because these databases have not been expanded since then. The U–Pb, Lu–Hf, and Sm–Nd datasets, on the other hand, have been moderately or significantly expanded, so the discussion provided in this chapter focuses on the data produced using these three isotopic systems as produced since 1996. Pb–Pb evaporation dates are also not considered because the geological accuracy of these dates, in and by themselves, is impossible to assess. We also make mention of the limited (but relevant) $\delta^{18}O_{Zrn}$ stable isotope results that have recently become available. Thus, the data used for the purposes of this chapter comes from the following sources (in chronologic order): Tassinari et al. (1996), Santos et al. (2000), Ibañez–Mejia et al. (2011), Bonilla–Pérez et al. (2013), Ibañez–Mejia (2014), Ibañez–Mejia et al. (2015), Cordani et al. (2016b), Veras et al. (2018). U–Pb results obtained from this compilation are listed in Table 1, along with the sample coordinates (in degrees, using the WGS84 datum), geographic locality (if known), rock–type that was analyzed, and their unique International Geo Sample Number (IGSN) identifier when available. Sm–Nd, Lu–Hf, and $\delta^{18}O_{Zrn}$ results obtained in this compilation are shown in Table 2, where only data obtained from samples with known U–Pb ages are listed and the quoted $^{143}Nd/^{144}Nd$, εNd, $^{176}Hf/^{177}Hf$, and εHf have been corrected to their initial values using the crystallization ages quoted in Tables 1, 2, and the decay constants of Lugmair & Marti (1978) and Söderlund et al. (2004).

Current models describing the growth and evolution of Amazonia indicate that, beginning at ca. 2.0 Ga, accretionary belts developed along the western margin of a cratonic nucleus that formed after the Transamazonian Orogeny. These accretionary belts are known as the Ventuari–Tapajós (ca. 2000–1800 Ma), Rio Negro–Juruena (ca. 1780–1550 Ma), and Rondonian–San Ignacio (ca. 1500–1300 Ma) (Cordani & Teixeira, 2007; Tassinari & Macambira, 1999). Continued soft–collision/accretion of these belts, driven by subduction–related processes, produced a very large "basement" in which granitoid rocks predominate, many of them with juvenile–like Nd isotopic signatures. Felsic volcanics are also widespread, and to date no clear evidence of Archean basement inliers within these tectonic provinces has been reported.

Recent geologic and geochronologic studies conducted in basement exposures found along the Caquetá, Inírida, Atabapo, and Orinoco Rivers (and vicinities) have greatly improved our understanding of the geology in eastern Colombia, thus allowing for a better interpretation of its evolution within the general tectonic framework of Amazonia and the western Guiana Shield. Outcrops along the Colombia–Venezuela border are key because they lie near the projected suture between the Ventuari–Tapajós and Rio Negro–Juruena Provinces as traced by Cordani & Teixeira (2007), thus providing an opportunity to test the predictions of their model and better understanding the nature and location of this boundary in the Guiana Shield. The Araracuara basement high is also of particular interest, mainly because it represents the westernmost basement exposure in eastern Colombia and thus allows evaluating the presence and/or location of potential Mesoproterozoic terranes and sutures in the western Guiana Shield. The sections below provide a brief summary of field observations from these two key areas, which are relevant for interpreting the geochronologic database compiled here.

2.1. Geology of the Araracuara Basement High, Caquetá River

The Araracuara High is an isolated basement exposure along the Caquetá River in SE Colombia (Figures 2, 3), which exposes a series of metasedimentary, igneous, and metaigneous rocks that uncomformably underlie mid–Paleozoic strata of the Araracuara Formation (Figure 4a, 4b). Based on field mapping and petrographic observations, the basement exposed here can be subdivided into at least four major units (Barrera, 1988; Galvis et al., 1979; Ibañez–Mejia, 2014): (i) A meta–(volcano)sedimentary unit composed predominantly by quartz–feldspar gneisses, with or without biotite, muscovite, and ± sillimanite (Figure 4a–c); (ii) equigranular and strongly

Table 1. Compilation of published geochronologic data from the westernmost Guiana Shield using modern U–Pb methods.

Sample name	Latitude	Longitude W	Locality (if know)	Rock type	Mean ± 2σ	Method	Reference	IGSN
Putumayo Basin basement								
Mandur–2 Melano	0° 55' 24.51'' N	75° 52' 34.09''	Putumayo Basin well	Orthogneiss	1602 ± 16	LA–ICP–MS	Ibañez–Mejia et al. (2011, 2015)	IEURI0014
Payara–1	2° 7' 31.35'' N	74° 33' 35.92''	Putumayo Basin well	Orthogneiss	1606 ± 6	LA–ICP–MS	Ibañez–Mejia et al. (2011, 2015)	IEURI0012
Araracuara basement high								
11MIAr–16	0° 36' 46.16'' S	72° 23' 39.86''	Caquetá River, Araracuara	Dolerite	102.5 ± 2.3	LA–ICP–MS	Ibañez–Mejia (2014)	IEURI0048
11MIAr–18	0° 37' 17.03'' S	72° 15' 29.24''	Caquetá River, Yarí Island	Porph. Syenogranite	1539 ± 20	LA–ICP–MS	Ibañez–Mejia (2014)	IEURI0049
11MIAr–22	0° 40' 8.28'' S	72° 5' 7.45''	Caquetá River, Peña Roja	Foliated Syenogranite	1716 ± 16	LA–ICP–MS	Ibañez–Mejia (2014)	IEURI0050
EP–2	0° 34' 41.37'' S	72° 23' 16.32''	Cañón del Diablo	Biotite gneiss	1721 ± 10	SHRIMP	Cordani et al. (2016b)	N.A.
11MIAr–07	0° 37' 0.89'' S	72° 23' 10.92''	Caquetá River, Araracuara	Orthogneiss	1731 ± 16	LA–ICP–MS	Ibañez–Mejia (2014)	IEURI0046
J–263	0° 40' 10.37'' S	72° 5' 26.16''	Caquetá River, Peña Roja	Syenogranite	1732 ± 17	LA–ICP–MS	Ibañez–Mejia et al. (2011)	N.A.
PR–3215	0° 10' 13.46'' S	72° 17' 36.63''	Araracuara	Syenogranite	1756 ± 8	LA–ICP–MS	Ibañez–Mejia et al. (2011)	N.A.
11MIAr–02			Caquetá River, Araracuara	Paragneiss	DZ	LA–ICP–MS	Ibañez–Mejia (2014)	IEURI0044
11MIAr–06	0° 37' 3.15'' S	72° 23' 2.52''	Caquetá River, Araracuara	Paragneiss	DZ	LA–ICP–MS	Ibañez–Mejia (2014)	IEURI0045
11MIAr–08	0° 35' 40.55'' S	72° 24' 30.07''	Cañón del Diablo	Paragneiss	DZ	LA–ICP–MS	Ibañez–Mejia (2014)	IEURI0047
PR–3228	0° 4' 5.85''N	72° 15' 33.76''	Mesai River	Paragneiss	DZ	LA–ICP–MS	Cordani et al. (2016b)	N.A.
Apaporis River, Vaupés Department, and vicinities								
AH–1231	1° 10' 33.6'' N	70° 11' 6.65''	Serranía Mitú	Monzogranite	1510 ± 26	LA–ICP–MS	Cordani et al. (2016b)	N.A.
AF–1	0° 2' 28.09'' N	67° 4' 3.15''	São Gabriel	Granite with titanite	1518 ± 25	ID–TIMS	Santos et al. (2000)	N.A.
PA–22	0° 48' 0'' N	69° 15' 0''	Papuri River	Granite	1521 ± 13	SHRIMP	Tassinari et al. (1996)	N.A.
AH–1419	0° 34' 35.19'' S	70° 15' 38.79''	Apaporis River	Monzogranite	1530 ± 21	LA–ICP–MS	Ibañez–Mejia et al. (2011)	N.A.
AH–1216	0° 59' 42.23'' N	69° 54' 37.31''	Vaupés River	Monzogranite	1574 ± 10	LA–ICP–MS	Ibañez–Mejia et al. (2011)	N.A.
PR–3092	0° 18' 57.74'' S	70° 39' 15.23''	Apaporis River	Syenogranite	1578 ± 27	LA–ICP–MS	Ibañez–Mejia et al. (2011)	N.A.
CJR–19	1° 0' 59.94'' S	69° 45' 24.35''	Apaporis River	Syenogranite	1593 ± 6	LA–ICP–MS	Ibañez–Mejia et al. (2011)	N.A.
UA–39	1° 12' 0'' N	69° 34' 60''	Vaupés River	Quartz–diorite	1703 ± 7	ID–TIMS	Tassinari et al. (1996)	N.A.
AH–1213A	0° 57' 25.59'' N	69° 57' 44.91''	Raudal Tucunare	Bt–Hnbd orthogneiss	1736 ± 19	LA–ICP–MS	Cordani et al. (2016b)	N.A.
PR–3001	1° 23' 2.76'' N	70° 36' 49.25''	Caño Cuduyari	Bt–chl gneiss	1769 ± 33	SHRIMP	Cordani et al. (2016b)	N.A.
HB–667	1° 5' 23.87'' N	69° 20' 51.41''	Raudal Cururu	Monzogranite	1778.8 ± 5.9	SHRIMP	Cordani et al. (2016b)	N.A.
MA44	1° 24' 7.2'' N	68° 5' 31.2''	Içana River	Diatexite	1788 ± 11	LA–ICP–MS	Veras et al. (2018)	N.A.
MA29	1° 27' 36'' N	68° 3' 3.6''	Içana River	Diatexite	1798 ± 11	LA–ICP–MS	Veras et al. (2018)	N.A.
MA21A	2° 9' 7.2'' N	68° 3' 28.8''	Peuá Creek	Metagranite	1813 ± 19	LA–ICP–MS	Veras et al. (2018)	N.A.

Table 1. Compilation of published geochronologic data from the westernmost Guiana Shield using modern U–Pb methods (*continued*).

Sample name	Latitude	Longitude W	Locality (if know)	Rock type	Mean ± 2σ	Method	Reference	IGSN
Apaporis River, Vaupés Department, and vicinities								
MS–63	0° 14' 13.32'' N	66° 39' 17.46''	Iã–Mirim River	Monzogranite	1810 ± 9	SHRIMP	Santos et al. (2000)	N.A.
J–42	1° 16' 41.35'' N	70° 6' 38.09''		Paragneiss	DZ	LA–ICP–MS	Cordani et al. (2016b)	N.A.
J–36	1° 24' 24.13'' N	70° 35' 28.37''		Paragneiss	DZ	LA–ICP–MS	Cordani et al. (2016b)	N.A.
Guainía Department and vicinities								
10MIGU–27	3° 13' 58.02'' N	68° 12' 12.54''		Bt–Hnbd monzogranite	1500 ± 15	LA–ICP–MS	Ibañez–Mejia (2014)	IEURI0037
PR–3141	3° 52' 32.1'' N	67° 55' 33.81''	Caño Cuauben	Biotite gneiss	1501 ± 10	SHRIMP	Cordani et al. (2016b)	N.A.
10MIGU–23	3° 45' 33.33'' N	67° 58' 31.56''		Biotite monzogranite	1504 ± 20	LA–ICP–MS	Ibañez–Mejia (2014)	IEURI0035
J–84	2° 59' 4.83'' N	68° 40' 21.97''	Raudal Morroco	Monzogranite	1507 ± 22	SHRIMP	Cordani et al. (2016b)	N.A.
10MIGU–26	3° 27' 28.15'' N	67° 58' 9.15''	Cerros de Mavecure	Biotite syenogranite	1509 ± 14	LA–ICP–MS	Ibañez–Mejia (2014)	IEURI0036
10MIGU–33	3° 51' 48.8'' N	67° 55' 8''		Biotite granite	1516 ± 16	LA–ICP–MS	Ibañez–Mejia (2014)	IEURI0043
J–98	2° 50' 40.32'' N	68° 38' 28.4''	Caño Nabuquen	Monzogranite	1752 ± 21	LA–ICP–MS	Cordani et al. (2016b)	N.A.
J–159	2° 20' 1.19'' N	68° 27' 24.15''	Serranía de Naquén	Tonalite	1770 ± 40	LA–ICP–MS	Cordani et al. (2016b)	N.A.
J–127	2° 11' 52.96'' N	68° 17' 47.98''	Caño Naquén, Guainía River	Tonalitic orthogneiss	1775.3 ± 7.7	SHRIMP	Cordani et al. (2016b)	N.A.
10MIGU–30	3° 47' 0.2'' N	67° 38' 2.43''	Caño Chaquita	Bt–Hnbd granite	1795 ± 15	LA–ICP–MS	Ibañez–Mejia (2014)	IEURI0040
10MIGU–31	3° 39' 28.1'' N	67° 32' 54.9''	Caño Chaquita	Biotite granite	1795 ± 18	LA–ICP–MS	Ibañez–Mejia (2014)	IEURI0041
J–199	2° 20' 32.99'' N	67° 13' 20.56''	Negro River	Bt–Hnbd orthogneiss	1796.1 ± 3.7	SHRIMP	Cordani et al. (2016b)	N.A.
10MIGU–32	3° 36' 59.01'' N	67° 34' 28.62''		Biotite granite	1797 ± 17	LA–ICP–MS	Ibañez–Mejia (2014)	IEURI0042
10MIGU–29	4° 1' 42.35'' N	67° 42' 17.27''		Bt–Hnbd monzogranite	1806 ± 17	LA–ICP–MS	Ibañez–Mejia (2014)	IEURI0039
10MIGU–28	3° 48' 16.3'' N	67° 50' 2''		Biotite syenogranite	1810 ± 16	LA–ICP–MS	Ibañez–Mejia (2014)	IEURI0038
6580–6085	3° 43' 60'' N	66° 40' 0''	Casiquiare River	Tonalite	1834 ± 18	SHRIMP	Tassinari et al. (1996)	N.A.
AH–1248	3° 39' 46.54'' N	67° 32' 43.31''			DZ	LA–ICP–MS	Cordani et al. (2016b)	N.A.
Orinoco River, Vichada Department, and vicinities								
10MIGU–03	6° 30' 24.99'' N	67° 1' 7.92''		Rapakivi granite	1388 ± 13	LA–ICP–MS	Ibañez–Mejia (2014)	IEURI0021
COL–21	5° 7' 54.1'' N	68° 6' 47.42''		Rapakivi granite	1392 ± 5	LA–ICP–MS	Bonilla–Pérez et al. (2013)	N.A.
COL–16	5° 29' 49.93'' N	67° 40' 28.19''		Rapakivi granite	1401 ± 4	LA–ICP–MS	Bonilla–Pérez et al. (2013)	N.A.
10MIGU–06	6° 22' 8.27'' N	67° 6' 41.07''		Rapakivi granite	1401 ± 14	LA–ICP–MS	Ibañez–Mejia (2014)	IEURI0023
10MIGU–05	6° 10' 23.21'' N	67° 23' 0.59''		Rapakivi granite	1402 ± 13	LA–ICP–MS	Ibañez–Mejia (2014)	IEURI0022
10MIGU–01	5° 14' 15.05'' N	67° 47' 48.89''		Rapakivi granite	1405 ± 12	LA–ICP–MS	Ibañez–Mejia (2014)	IEURI0019

Table 1. Compilation of published geochronologic data from the westernmost Guiana Shield using modern U–Pb methods (*continued*).

Sample name	Latitude	Longitude W	Locality (if know)	Rock type	Mean ± 2σ	Method	Reference	IGSN
Orinoco River, Vichada Department, and vicinities								
10MIGU–02	5° 21' 3.7" N	67° 41' 33.41"		Rapakivi granite	1408 ± 14	LA–ICP–MS	Ibañez–Mejia (2014)	IEURI0020
10MIGU–11	6° 56' 22.43" N	66° 31' 6.01"		Biotite granite	1424 ± 21	LA–ICP–MS	Ibañez–Mejia (2014)	IEURI0025
10MIGU–10	6° 51' 32.47" N	66° 36' 19.34"		Biotite leucogranite	1984 ± 18	LA–ICP–MS	Ibañez–Mejia (2014)	IEURI0024
10MIGU–12	7° 5' 37.63" N	66° 29' 49.1"		Biotite monzogranite	1989 ± 21	LA–ICP–MS	Ibañez–Mejia (2014)	IEURI0026

foliated biotite orthogneisses exposed in the Cañón del Diablo gorge and near Sumaeta and Mariñame islands (Figure 4d); (iii) coarsely porphyritic and undeformed syenogranites, best exposed near Yarí island and the Yarí River junction (Figure 4e, 4f); (iv) a younger and less deformed metasedimentary sequence that uncomformably overlies the gneissic/granitic basement, known as the La Culebra unit –not extensively exposed in map area of Figure 2–, and whose low–grade metamorphism distinguishes from the Paleozoic sedimentites of the Araracuara Formation. The first two units (i.e., paragneisses and orthogneisses) have been collectively mapped as the 'Araracuara Gneiss' unit (Figure 2). All igneous/metaigneous units are pervasively intruded by granitic dikes and sills, many of which have coarsely pegmatitic textures (e.g., Figure 4g), and a later generation of dikes and sills of doleritic composition (e.g., Figure 4h).

Samples from this uplift have been dated using zircon U–Pb geochronology by Cordani et al. (2016b), Ibañez–Mejia (2014), and Ibañez–Mejia et al. (2011), who have analyzed the (meta)granitoids outcropping along the Yarí River (sample PR–3215), the Caquetá River near the Sumaeta (J–263 and 11MIAr–22), and Yarí (11MIAr–18) islands, as well as samples taken along the Caquetá River closer to the town of Araracuara, collected from ortho– (EP–2 and 11MIAr–07) and paragneisses (11MIAr–02, –06, and –08) of the Araracuara Gneiss unit in the Cañón del Diablo gorge. These studies have found the orthogneisses in the region to yield exclusively Paleoproterozoic (ca. 1.72 to 1.76 Ga) ages for the igneous crystallization of their protoliths, while paragneisses yield unimodal detrital zircon age distributions with maximum depositional ages of around 1.73 Ga. Ibañez–Mejia (2014) interpreted the Araracuara Gneiss as reflecting: (i) A metamorphosed volcano–sedimentary sequence whose protoliths formed in a forearc basin associated with a Paleoproterozoic arc; and (ii) that these basins were rapidly buried, intruded by granitoid magmas and metamorphosed at an age that must be younger (but indistinguishable within LA–ICP–MS U–Pb age uncertainty) relative to their timing of sedimentation. No ages of metamorphism from zircon recrystallization fronts or overgrowths have yet been determined from the Araracuara Gneiss. Some of the porphyritic and unmetamorphosed syenogranites in the area, however, yield ca. 1.54 Ga U–Pb crystallization ages, which constrain the regional metamorphism that affected the Araracuara Gneiss to be older than this event.

A sample from a doleritic dike intruding the Araracuara Gneiss (11MIAr–16) dated by Ibañez–Mejia (2014) produced an Albian age of 102.5 ± 2.3 Ma, which indicates that mid Cretaceous magmatism has affected the continental interior of Colombia as far inland as Araracuara. The Cretaceous age of this dike was confirmed by Sm–Nd whole–rock isotopic analyses of the same sample, whose highly radiogenic initial $^{143}Nd/^{144}Nd$ precludes derivation from the Proterozoic mantle.

Locations of all samples that have been studied from the Araracuara High are shown in Figure 3 and their coordinates listed in Table 1. Only two granitic samples collected along the Caquetá River E of Araracuara have been analyzed for Lu–Hf isotopes in zircons following U–Pb dating, and only three Sm–Nd isotopic results from whole–rock aliquots are thus far available (Table 2).

2.2. Geology of Guainía and Vichada Near the Colombia–Venezuela Border

The most extensive outcrops of Precambrian basement in Colombia are located in the eastern and southeastern portions of the Vichada and Guainía Departments (Figure 2), along the Orinoco, Guaviare, Inírida, Atabapo, Guainía, and Negro River basins (Gómez et al., 2017). Samples dated by U–Pb methods in this region, from the studies of Bonilla–Pérez et al. (2013), Cordani et al. (2016b), and Ibañez–Mejia (2014) are mainly from outcrops located around the Orinoco, Inírida, and Atabapo Rivers. From oldest to youngest, the basement in this area is comprised by: (i) Volcanic and intrusive rocks of the Cuchivero magmatic belt (Gibbs, 1987; Teixeira et al., 2002), with crystallization ages ca. 1.99 Ga and thus presumably belonging to a broader magmatic event in the Guiana Shield known as the Orocaima event (Reis et al., 2000), which in NW Venezuela is dominantly comprised by coarse– and

Table 2. Compilation of published Sm–Nd, Lu–Hf, and O isotopic data from the westernmost Guiana Shield.

Sample name	$^{143}Nd/^{144}Nd \pm 2SE_{(t)}$	$\varepsilon Nd_{(t)} \pm 2SE$	U–Pb cryst. age	2–stage T_{DM} (Ga)	Reference	IGSN
Putumayo Basin basement Payara–1	0.510638 ± 8	+1.50 ± 0.16	1606 Ma	2.01	Ibañez–Mejia et al. (2015)	IEURI0012
Araracuara basement high 11MIAr–16	0.512722 ± 14	+4.14 ± 0.28	103 Ma	0.52	Ibañez–Mejia (2014)	IEURI0048
11MIAr–22	0.510500 ± 24	+1.60 ± 0.47	1716 Ma	2.09	Ibañez–Mejia (2014)	IEURI0050
EP–2	0.510418	+0.12	1721 Ma	2.24	Cordani et al. (2016b)	N.A.
Apaporis River, Vaupés Department, and vicinities						
AH–1231	0.510639	–0.91	1510 Ma	2.17	Cordani et al. (2016b)	N.A.
AH–1213A	0.510382	–0.20	1736 Ma	2.28	Cordani et al. (2016b)	N.A.
PR–3001	0.510388	+0.76	1769 Ma	2.22	Cordani et al. (2016b)	N.A.
HB–667	0.510329	–0.15	1779 Ma	2.31	Cordani et al. (2016b)	N.A.
Guainía Department and vicinities						
PR–3141	0.510489	–4.08	1501 Ma	2.48	Cordani et al. (2016b)	N.A.
J–84	0.510533	–3.07	1507 Ma	2.38	Cordani et al. (2016b)	N.A.
J–98	0.510331	–0.79	1752 Ma	2.36	Cordani et al. (2016b)	N.A.
J–159	0.510368	+0.41	1770 Ma	2.25	Cordani et al. (2016b)	N.A.
J–127	0.510326	–0.30	1775 Ma	2.33	Cordani et al. (2016b)	N.A.
J–199	0.510301	–0.25	1796 Ma	2.34	Cordani et al. (2016b)	N.A.

Sample name	$^{176}Hf/^{177}Hf \pm 2SD_{(t)}$	$\varepsilon Hf_{(t)} \pm 2SD$	U–Pb cryst. age	$\delta^{18}O \pm 2SD$ (‰)	Reference	IGSN
Putumayo Basin basement Mandur–2 Melano	0.281974 ± 42 (n=18)	+7.6 ± 1.5	1602 Ma	5.43 ± 0.23 (n=22)	Ibañez–Mejia et al. (2015)	IEURI0014
Payara–1	0.281796 ± 70 (n=11)	+0.8 ± 2.5	1606 Ma	ca. 9.0 to 9.4	Ibañez–Mejia et al. (2015)	IEURI0012
Araracuara basement high 11MIAr–18	0.281803 ± 46 (n=6)	–0.1 ± 1.5	1539 Ma	N.A.	Ibañez–Mejia (2014)	IEURI0049
11MIAr–22	0.281738 ± 59 (n=11)	+1.7 ± 2.0	1716 Ma	N.A.	Ibañez–Mejia (2014)	IEURI0050
Guainía Department and vicinities						
10MIGU–27	0.281686 ± 76 (n=16)	–5.1 ± 2.7	1500 Ma	8.95 ± 0.60 (n=16)	Ibañez–Mejia (2014)	IEURI0037
10MIGU–23	0.281696 ± 37 (n=16)	–4.7 ± 1.3	1504 Ma	8.41 ± 0.67 (n=14)	Ibañez–Mejia (2014)	IEURI0035
10MIGU–26	0.281667 ± 54 (n=15)	–5.6 ± 1.9	1509 Ma	9.29 ± 0.50 (n=16)	Ibañez–Mejia (2014)	IEURI0036
10MIGU–33	0.281702 ± 40 (n=16)	–4.2 ± 1.4	1516 Ma	8.27 ± 0.39 (n=12)	Ibañez–Mejia (2014)	IEURI0043
10MIGU–30	0.281634 ± 54 (n=15)	–0.2 ± 1.9	1795 Ma	8.37 ± 0.59 (n=18)	Ibañez–Mejia (2014)	IEURI0040
10MIGU–31	0.281658 ± 58 (n=15)	+0.6 ± 2.1	1795 Ma	7.09 ± 0.31 (n=13)	Ibañez–Mejia (2014)	IEURI0041
10MIGU–32	0.281614 ± 50 (n=15)	–0.9 ± 1.8	1797 Ma	7.63 ± 0.53 (n=17)	Ibañez–Mejia (2014)	IEURI0042
10MIGU–29	0.281637 ± 84 (n=17)	+0.2 ± 3.0	1806 Ma	8.52 ± 0.37 (n=12)	Ibañez–Mejia (2014)	IEURI0039
10MIGU–28	0.281633 ± 68 (n=16)	+0.1 ± 2.4	1810 Ma	7.69 ± 0.29 (n=13)	Ibañez–Mejia (2014)	IEURI0038
Orinoco River, Vichada Department, and vicinities						
10MIGU–03	0.281814 ± 50 (n=15)	–3.2 ± 1.8	1388 Ma	6.23 ± 0.30 (n=12)	Ibañez–Mejia (2014)	IEURI0021
10MIGU–06	0.281776 ± 50 (n=15)	–4.2 ± 1.8	1401 Ma	6.50 ± 0.37 (n=12)	Ibañez–Mejia (2014)	IEURI0023
10MIGU–05	0.281782 ± 57 (n=16)	–4.0 ± 2.0	1402 Ma	6.36 ± 0.26 (n=7)	Ibañez–Mejia (2014)	IEURI0022
10MIGU–01	0.281784 ± 84 (n=18)	–3.8 ± 3.0	1405 Ma	6.32 ± 0.28 (n=11)	Ibañez–Mejia (2014)	IEURI0019
10MIGU–02	0.281771 ± 77 (n=7)	–4.2 ± 2.8	1408 Ma	5.69 ± 0.55 (n=7)	Ibañez–Mejia (2014)	IEURI0020
10MIGU–11	0.281800 ± 72 (n=16)	–2.8 ± 2.6	1424 Ma	5.26 ± 0.13 (n=10)	Ibañez–Mejia (2014)	IEURI0025
10MIGU–10	0.281555 ± 51 (n=13)	+1.4 ± 1.8	1984 Ma	4.89 ± 0.37 (n=12)	Ibañez–Mejia (2014)	IEURI0024
10MIGU–12	0.281540 ± 86 (n=15)	+0.9 ± 3.1	1989 Ma	4.73 ± 0.39 (n=13)	Ibañez–Mejia (2014)	IEURI0026

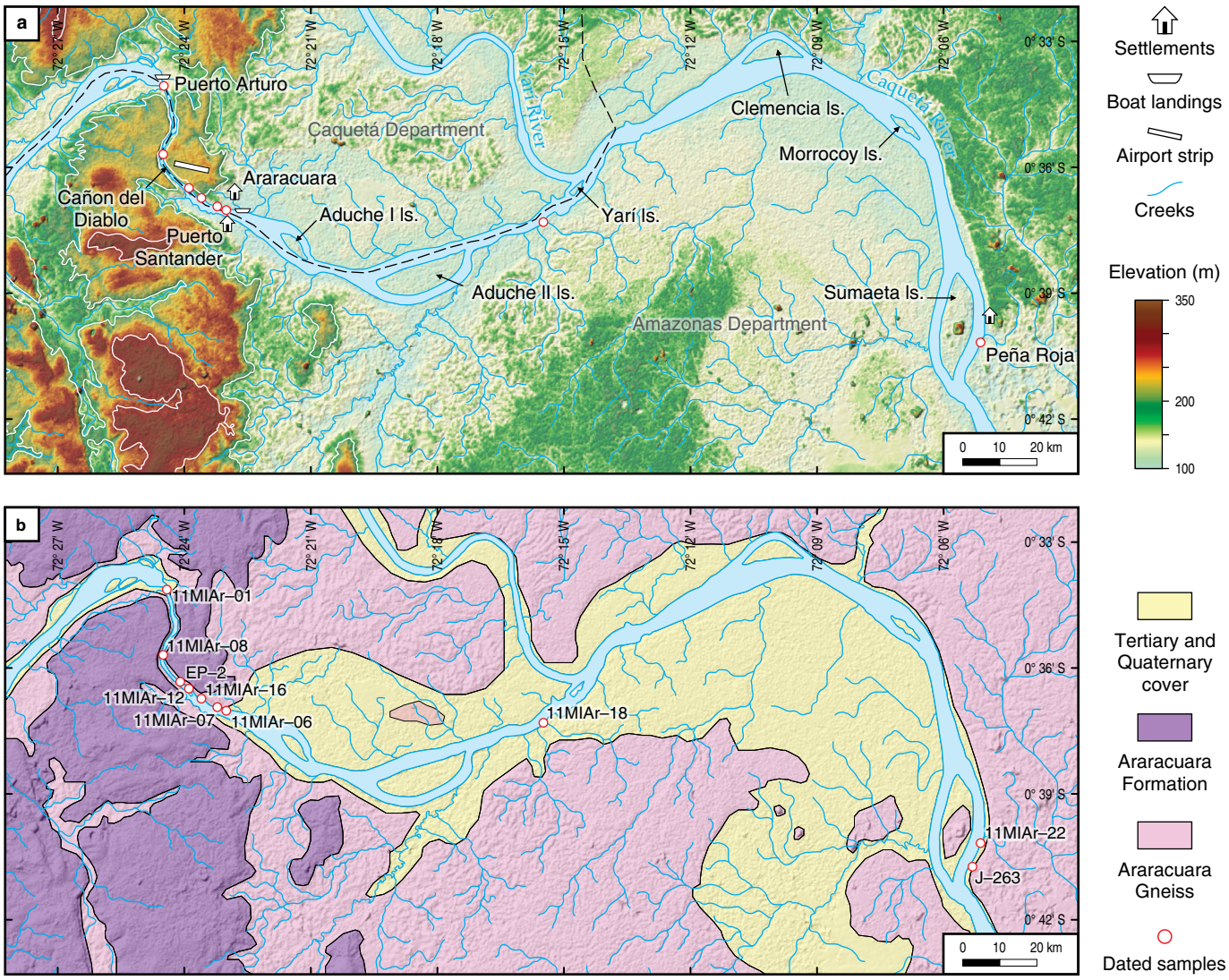

Figure 3. Topographic **(a)** and geologic **(b)** map of the Araracuara region, showing the location of samples collected and analyzed by Cordani et al. (2016b), Ibañez–Mejia (2014), and Ibañez–Mejia et al. (2011). (Is.) Island.

fine–grained biotite granitoids (e.g., Figure 5a, 5b); (ii) intermediate and granitic orthogneisses which are widespread along the Atabapo and Ventuari Rivers (e.g., Figure 5c) and yield igneous crystallization ages ca. 1.8 Ga like those of the Cauaburi Complex and Taiuaçu–Cauera diatexite in NW Brasil (Almeida et al., 2013; Veras et al., 2018). In addition to their penetrative gneissic fabric, these orthogneisses show local evidences of intense mylonitic deformation (Figure 5d); (iii) coarsely porphyritic intrusives like those that make up the "Cerros de Mavecure" inselbergs (Figure 5e, 5f) which yield U–Pb crystallization ages ca. 1.5 Ga. These intrusives can locally contain abundant metasedimentary enclaves (Figure 5g), exhibit primary magmatic fabrics denoted by alignment of orthoclase phenocrysts (Figure 5h), or have more massive, equigranular textures (Figure 5i, 5j); (iv) the Parguaza intrusive complex, which is mostly comprised by granitoids with rapakivi textures that yield U–Pb crystallization ages ca. 1.4 Ga. Outcrops of the Parguaza complex are common along the Orinoco River in Colombia and Venezuela (Figure 5k), but are best exposed in large inselbergs to the E and NE of Puerto Ayacucho (Figure 5l). Most outcrops of this unit are characterized by granitoids with fine– to coarse–grained rapakivi textures (e.g., Figure 5m, 5n).

In addition to the crystallization ages described above, Cordani et al. (2016b) obtained whole–rock Sm–Nd isotopic data from six of their dated samples, and Ibañez–Mejia (2014) obtained Lu–Hf and $\delta^{18}O_{Zrn}$ isotopic results for 17 samples from this region (Table 2). These isotopic datasets, in combination with the U–Pb dates, allow to better understand the sources of these magmas and make inferences about the processes involved in their generation and possible tectonic setting.


a


b


c


d


e


f


g


h

Figure 4. Field photographs of outcrops in the Araracuara basement high. **(a)** Caquetá river exiting through the eastern end of the Cañón del Diablo gorge, near locality 11MIAr–12 of Figure 3b; Proterozoic metasedimentary rocks of the Araracuara Gneiss appear in the foreground and Paleozoic sedimentary rocks of the Araracuara Formation in the background. **(b)** The 'Great Unconformity' of the Colombian Amazon: Paleozoic rocks of the Araracuara Formation overlie metasedimentary basement of the Araracuara Gneiss in the western end of the Cañón del Diablo gorge, near Puerto Arturo, Caquetá (locality 11MIAr–01 of Figure 3b). **(c)** Detail of layered biotite–rich and biotite–poor quartz–plagioclase metasedimentary gneisses of the Araracuara Gneiss unit, injected by coarse–grained quartz veins; sampling location 11MIAr–08, dip direction of foliation plane is 170/28. **(d)** Outcrop of foliated biotite monzogranite along the shoreline of the Caquetá River, near Sumaeta island in sampling locality 11MIAr–22 of Figure 3b. **(e)** Outcrop of coarsely porphyritic biotite monzogranite along the shoreline of the Caquetá River, near the junction of the Yarí River (sampling locality 11MIAr–18). **(f)** Detail of coarsely porphyritic biotite monzogranite in sampling locality 11MIAr–18, preserving primary magmatic fabric. **(g)** Pegmatitic dikes cross–cutting metasedimentary gneisses of the Araracuara Gneiss, near locality 11MIAr–12 of Figure 3b. **(h)** Cretaceous dolerite dike intruding metasedimentary rocks of the Araracuara Gneiss; sampling locality 11MIAr–16.

3. Discussion

3.1. It Is Time to Part with the Concept of a 'Mitú Migmatitic Complex'

The term "Mitú Migmatitic Complex" (MMC) was proposed by Galvis et al. (1979) to group all Proterozoic rocks in eastern Colombia stratigraphically underlying the so–called La Pedrera Formation. The original definition of the MMC included "metapsamites and metapelites, mafic and quartzofeldspathic metaigneous, blastomylonites, and migmatitic granitoid rocks belonging to the Guiana Shield". This definition might have been adequate in the late seventies, when exploratory mapping in the area was just starting to be performed, geochronologic information was unavailable, and modern concepts of continental construction by tectonic processes were arguably still in their infancy. However, this nomenclature results inaccurate and unpractical now, mainly because: (i) Evidently not all Precambrian rocks exposed in eastern Colombia and encompassed within this denomination are 'migmatitic' in nature (Figures 4, 5); and (ii) the growing geochronologic and isotopic database for the basement of eastern Colombia has started to shed light into the diversity of magmatic crystallization ages and possible orogenic events found in this geographically extensive region (see following sections).

Although still limited, the data compiled here allows distinct age and isotopic basement domains to be recognized and major tectonic boundaries to be sketched. Therefore, under the light of the currently available data, and with the prospect of much new geochronologic research to come, we consider the term Mitú Migmatitic Complex to be now obsolete and urge the geological community to abandon its usage, other than for historic purposes. Although it is not the objective of this chapter to propose new stratigraphic nomenclature, we believe future research efforts should be aimed at adopting a more accurate and flexible one, in line with modern geochronologic and petrologic research in the area. Using modern geochronologic and geochemical methods, it is anticipated that even individual arc sequences in this region can be identified and mapped with some detail in the future (e.g., Carneiro et al., 2017). The following sections will describe the main trends that stand out from the available geochronologic and isotopic data, and highlight recent efforts made towards adopting a modern tectonostratigraphic scheme for the basement of eastern Colombia.

3.2. Distribution of Proterozoic U–Pb Zircon Crystallization Ages in the Western Guiana Shield

The zircon U–Pb geochronologic database of eastern Colombia and adjoining regions in Venezuela and Brasil now consists of 57 published samples dated using modern methods (ID–TIMS, SHRIMP, and/or LA–ICP–MS; see Table 1 for a summary). Results from 46 of these samples interpreted as igneous crystallization ages of magmatic rocks, migmatitic leucosomes, or igneous protoliths of orthogneisses, are shown as a rank–order plot in Figure 6 and grouped by broad geographic regions. From southwest to northeast, the geographic areas used for grouping of ages are as follows: (i) Buried basement of the Putumayo Basin, which for the purposes of this chapter only includes Paleoproterozoic and early to mid–Mesoproterozoic protolith crystallization ages of orthogneisses in this region but excludes younger Proterozoic ages associated to the Putumayo orogenic cycle (discussed in Ibañez–Mejia, 2020); (ii) exposed basement of the Araracuara High, which includes all basement exposures along the Caquetá and Yarí Rivers; (iii) exposed basement outcrops along the Apaporis River, the Vaupés River, and elsewhere in the Vaupés Department and surrounding regions in Brasil (labeled 'Vaupés', for simplicity); (iv) exposed basement along the Inírida and Atabapo Rivers, elsewhere in the Guainía Department and neighboring areas in Venezuela (labeled 'Guainía'); and (v) exposed basement along the Orinoco River, the Vichada Department, and neighboring areas in Venezuela (labeled 'Orinoco').

In general, the current U–Pb geochronologic database indicates that igneous rocks from the Precambrian basement of the westernmost Guiana Shield predominantly crystallized during the Paleo– and Mesoproterozoic, between ca. 1.99 and 1.38 Ga. The oldest rock that has been dated within Colombian territory to this date is a fine–grained pink syenogranite exposed at 'Ce-

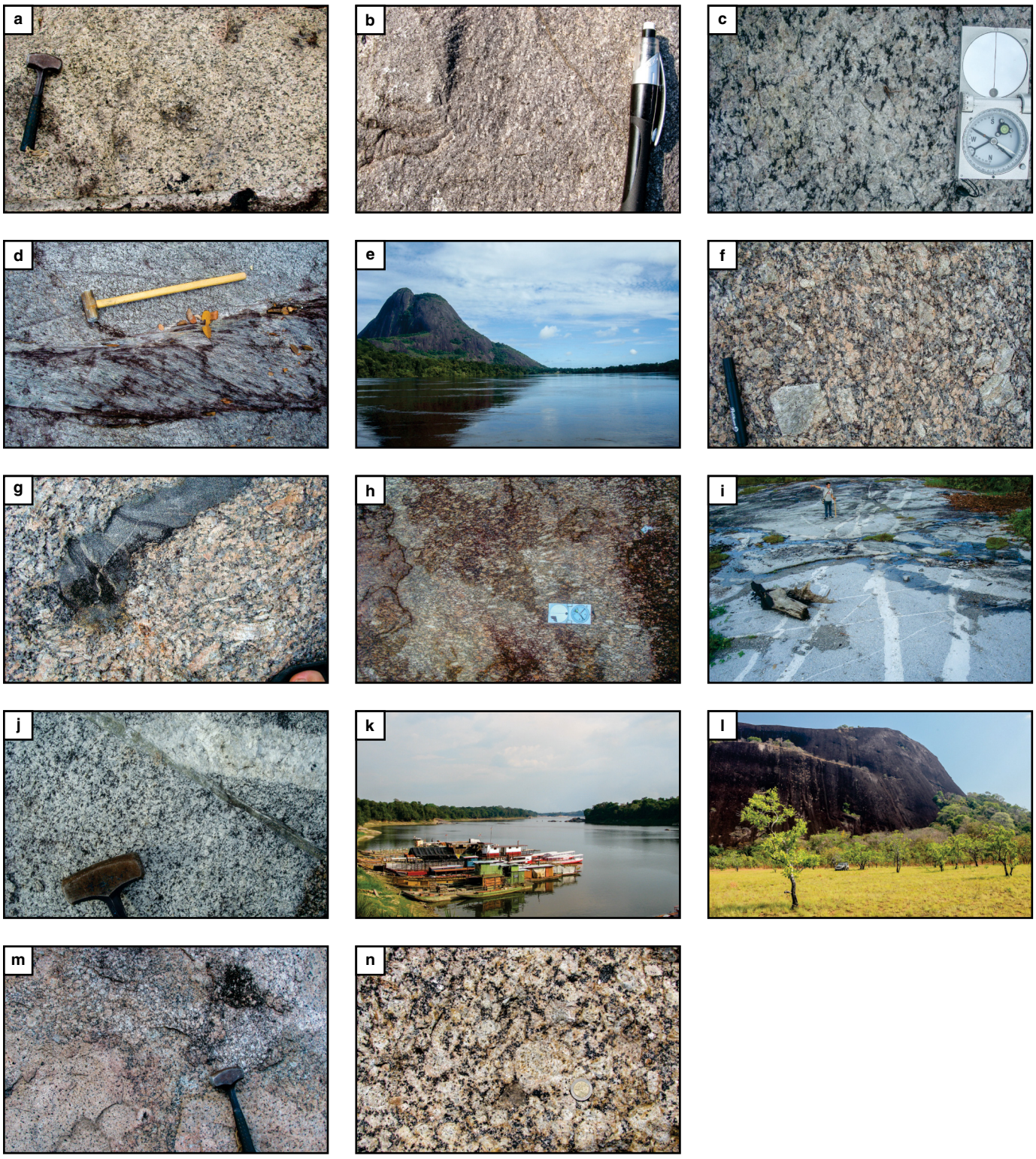

rro Vitina' in Guainía, with a U–Pb crystallization age of 1810 ± 16 Ma (sample 10MIGU–28 in Table 1), although the potential for Cuchivero–like (ca. 2.0 Ga) igneous rocks to be present in the Vichada Department, or older rocks elsewhere, still remains to be explored in more detail.

The geochronologic dataset summarized in Figure 6 defines at least four broad age clusters, which are representative of major magmatic episodes that have shaped the westernmost Guiana Shield; these are: (i) Ages around 1.99 Ga, obtained from felsic igneous rocks of the Cuchivero magmatic belt and likely belonging to the Orocaima event; (ii) a broad group of mid Paleoproterozoic ages, ranging from 1.84 to 1.72 Ga and mostly representative of igneous (protolith) crystallization ages from weakly– to strongly–foliated orthogneisses; (iii) a broad group

Figure 5. Field photographs of outcrops in the Guainía and Vichada Departments (and vicinities), mostly taken from outcrops along the Inírida, Atabapo, and Orinoco Rivers. **(a)** Coarse–grained, foliated biotite monzogranites of the Cuchivero Belt in Venezuela; sampling locality 10MIGU–14 (not shown in Figure 2). **(b)** Very fine–grained biotite leucogranites of the Cuchivero Belt in Venezuela; sampling locality 10MIGU–10. **(c)** Detail of ca. 1.8 Ga biotite orthogneisses from the Caño Chaquita creek tributary of the Atabapo River, defining a metamorphic foliation striking ca. 40° (azimuth); sampling location 10MIGU–31. **(d)** Meter–scale S–C mylonite cross–cutting the metamorphic foliation of 1.8 Ga orthogneisses; Caño Chaquita creek, near sampling location 10MIGU–31. **(e)** 'Cerros de Mavecure' inselbergs along the Inírida River. **(f)** Strongly porphyritic biotite syenogranite from the base of Cerros de Mavecure; sampling location 10MIGU–26. **(g)** Partially resorbed metasedimentary enclave in high $\delta^{18}O_{zrn}$ 1.5 Ga porphyritic syenogranites of the Inírida River, near Cerros de Mavecure. **(h)** Porphyritic biotite syenogranites from the raudal Qualé, defining a magmatic orientation fabric striking ca. 140° (azimuth); sampling location 10MIGU–27. **(i)** Massive biotite granites from the 'Laja los Libertadores', near Puerto Inírida, intruded by leucocratic granite dikes; sampling location 10MIGU–33. Geologist Zeze AMAYA for scale. **(j)** Detail of biotite granites of the 'Laja los Libertadores', crosscut by discrete shear zones forming centimeter–scale cataclasites. **(k)** Exposures of the Parguaza Complex along the Orinoco River near Samariapo. Left (east) margin of the river is Venezuelan territory and right (west) margin is Colombian; photo near sampling locality 10MIGU–01. **(l)** Inselbergs of the Parguaza Complex NE of Puerto Ayacucho, Venezuela; sampling locality 10MIGU–06. **(m)** Medium–grained rapakivi granites of the Parguaza Complex; sampling locality 10MIGU–06. **(n)** Coarse–grained rapakivi granites of the Parguaza Complex; sampling locality 10MIGU–03.

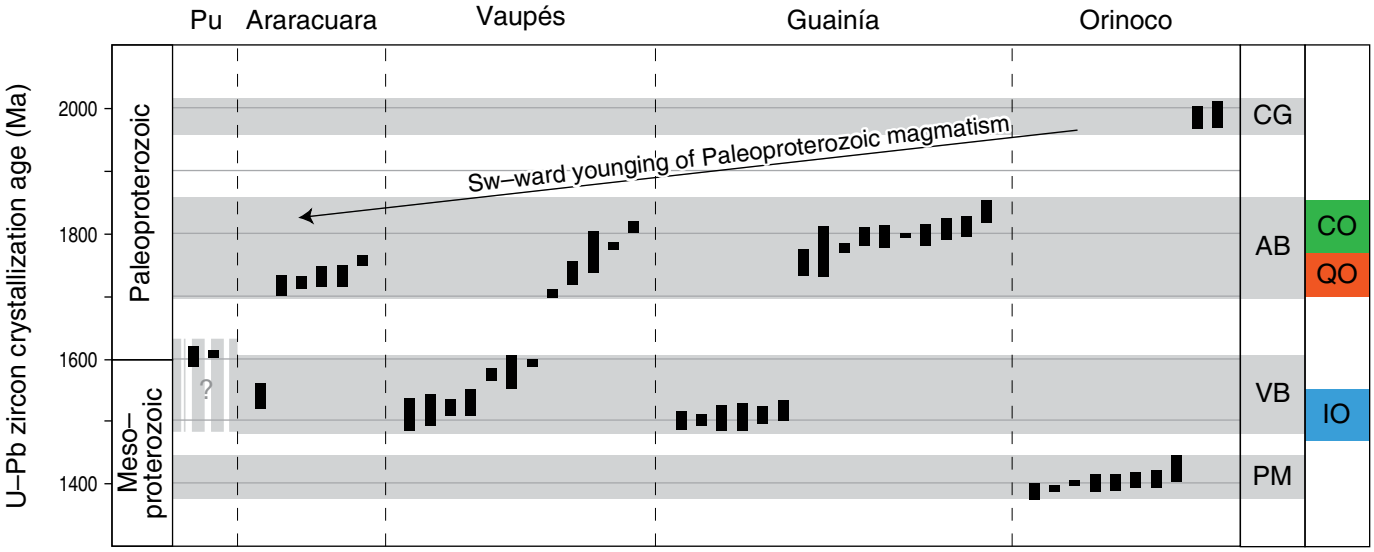

Figure 6. Rank–order plot, organized by geographic region, of the U–Pb geochronologic database available for the westernmost Guiana Shield. (Pu) includes orthogneiss protolith crystallization ages from the basement of the Putumayo Foreland Basin; (Araracuara) includes all samples dated from the Araracuara basement high; (Vaupés) includes all samples dated from the Apaporis River, Vaupés Department, and neighboring regions in Brasil; (Guainía) includes all samples dated from the Inírida and Atabapo Rivers, the Guainía Department, and neighboring regions in Venezuela; (Orinoco) includes all samples dated from the Orinoco River, the Vichada Department, and neighboring regions in Venezuela. (CG) Cuchivero Granites; (AB) Atabapo Belt; (VB) Vaupés Belt; (PM) Parguaza Massif, are after Cordani et al. (2016b). (CO) Cauaburi Orogeny; (QO) Querari Orogeny; (IO) Içana Orogeny, are after Almeida et al. (2013).

of early Mesoproterozoic ages, ranging from 1.59 to 1.50 Ga and mostly representing crystallization ages of porphyritic and/or unmetamorphosed granitoids; and (iv) mid Mesoproterozoic ages defining a tight cluster from 1.42 to 1.39 Ga, associated with the emplacement of the rapakivi granite of the Parguaza Massif.

The U–Pb data as compiled here and shown in Figure 6 confirms that widespread magmatic events coeval with what Cordani et al. (2016b) called the 'Atabapo' and 'Vaupés' Belts, with ages around 1.8 and 1.5 Ga, respectively, are indeed of great importance throughout the region. In NW Brasil, crystallization ages between ca. 1.81 and 1.75 Ga have been described for the Cumati, Cauaburi, and Querari Complexes and the Taiuaçu–Cauera diatexite; these dates have been interpreted to define the Cauaburi and Querari Orogenies (Figure 6; Almeida et al., 2013; Veras et al., 2018), whereas the younger ca. 1.5 Ga intrusives have been associated with the Içana Orogeny (Almeida et al., 2013). These orogenic events proposed in Brazilian territory have been inferred as having taken place within a series of accretionary orogens, characterized by arc–related magmatism and soft collision events along the western margin of the proto–Amazonian Craton (Almeida et al., 2013).

Similarly to the tectonic history proposed for the Cauaburi, Querari, and Içana Orogenies, Cordani et al. (2016b) proposed that the Atabapo and Vaupés Belts in eastern Colombia also

reflect the successive construction of accretionary belts younging from northeast to southwest, stacked against proto–Amazonia during a long–lived convergent margin characterized by subduction–related magmatism and tectonism. What remains unclear, however, is whether these regional magmatic episodes are indeed representative of distinct crust–forming events that affected two separate geographic regions (i.e., a dominantly ca. 1.8 Ga accretionary belt in Guainía and a ca. 1.55 Ga one in Vaupés and Caquetá), or if the entire region consists essentially of Paleoproterozoic basement that was later affected by Mesoproterozoic post–tectonic or anorogenic magmatism (as previously suggested by Celada et al., 2006, and Kroonenberg & Reeves, 2011). Because the current isotopic and geochronologic database cannot unequivocally discard either of these two interpretations (see section 3.3), throughout the rest of this chapter we will consider both hypotheses as plausible and indicate that these should be the focus of continued research.

The U–Pb geochronologic data of Figure 6 shows that Paleo– and Mesoproterozoic magmatic events are not systematically clustered by geographic region as a function of their age, but rather that Paleoproterozoic basement rocks, which are typically found in the field as strongly foliated orthogneisses, are intruded throughout all eastern Colombia by Mesoproterozoic plutons. These younger ca. 1.59 to 1.38 Ga intrusives are typically less (ductilely) deformed or undeformed, and commonly exhibit strongly porphyritic (Figures 4f, 5f), rapakivi (Figure 5m, 5n), or fine–grained subvolcanic textures, with or without preservation of primary magmatic fabrics (e.g., Figure 4g, 4h). Thus, while it is clear that the Paleoproterozoic basement has been strongly deformed at mid– to high–temperatures and under high–strain conditions, it is not yet clear, but unlikely, that the Mesoproterozoic plutons have experienced a similar high–temperature deformation history.

Recently, Cordani et al. (2016b) interpreted the ca. 1.75 Ga orthogneisses in the Araracuara High as Paleoproterozoic inliers included within a Mesoproterozoic orogen. However, considering the more complete U–Pb database of Figure 6, an alternative interpretation of these data and the field observations is that the relatively undeformed ca. 1.55 Ga granitoids in Araracuara may represent post–tectonic intrusives emplaced within an older (orogenic) Paleoproterozoic basement. It is also tempting to interpret from Figure 6 that, while the ages of Paleoproterozoic magmatism become progressively younger from NE (Orinoco) to SW (Araracuara and Putumayo), thus possibly indicating the direction of arc migration throughout this period, the ages of Mesoproterozoic magmatism appear to young in the opposite direction. This migration of Mesoproterozoic magmatism towards the cratonic interior so far inland is unlike a trend that could be generated by arc–related processes, and could instead be the result of post–tectonic or anorogenic magmatic centers developing throughout the area during this time period. We note, however, that these two alternatives are difficult to disentangle using the currently available geochronologic data alone, so future research efforts aimed at testing these two hypotheses for the origin of the 'Atabapo' and 'Vaupés' magmatism will prove key for better understanding the geological evolution of eastern Colombia.

3.3. Zircon Lu–Hf and Whole–Rock Sm–Nd Constraints on Crustal Evolution

Whole–rock Sm–Nd isotopic measurements have been reported and compiled by Cordani et al. (2016b) and Lu–Hf isotopic compositions of zircon reported by Ibañez–Mejia (2014) and Ibañez–Mejia et al. (2015). A summary of all available results for both isotopic systems is presented in Table 2. In addition, $\delta^{18}O$ isotopic compositions of zircons also analyzed by U–Pb and Lu–Hf were reported for the samples studied by Ibañez–Mejia (2014) and Ibañez–Mejia et al. (2015), and are also summarized in Table 2.

Figure 7a summarizes the available Lu–Hf isotopic data available for the area, shown as mean initial $^{176}Hf/^{177}Hf$ compositions as a function of U–Pb crystallization age. In isotope–ratio vs. age space, epsilon Hf compositions (thin dashed lines) as a function of age can simply be plotted as deviations from the time–dependent chondritic reference value (thick blue line), such that both isotope–ratio and εHf values can be presented in the same diagram. This type of plot has the benefit of retaining the slope of trends in $^{176}Hf/^{177}Hf$ vs. time, which can be readily associated to apparent $^{176}Lu/^{177}Hf$ compositions of the source and/or used to easily identify the effects of zircon Pb–loss in zircon Hf data (see discussion in Ibañez–Mejia et al., 2015). Superimposed to this plot are also iso–T_{DM} contours (red thin lines) for various apparent depleted mantle 'extraction ages' (or mean crustal residence times), calculated here using the $^{176}Lu/^{177}Hf$ isotopic composition of bulk global subducted sediments (GLOOS; Plank & Langmuir, 1998) as an average composition of the bulk exposed continental crust. The Lu/Hf composition of GLOOS has an intermediate value between the bulk and lower continental crust values of Hawkesworth et al. (2010), and thus provides a good approximation of average–crust and is possibly more representative. The Mud Tank (MT) and R33 bars shown in the bottom left corner of Figure 7a reflect the external reproducibility (at 2 SD) of the $^{176}Hf/^{177}Hf$ measurements for low–rare–earth element (REE) and high–REE zircon, respectively (see Ibañez–Mejia et al., 2015 for more details) and provide a good estimate for uncertainty of mean values reported for samples.

Most of the existing zircon Lu–Hf data yield mean initial $^{176}Hf/^{177}Hf$ compositions at time of crystallization with equivalent $\varepsilon Hf_{Zrn} \leq +2$ (Figure 7a). The only exception to this generalization are zircon cores from the igneous protolith of ortho–amphibolites retrieved from the basement of the Mandur–2 well in the Putumayo basin, which have a mean εHf_{Zrn} value

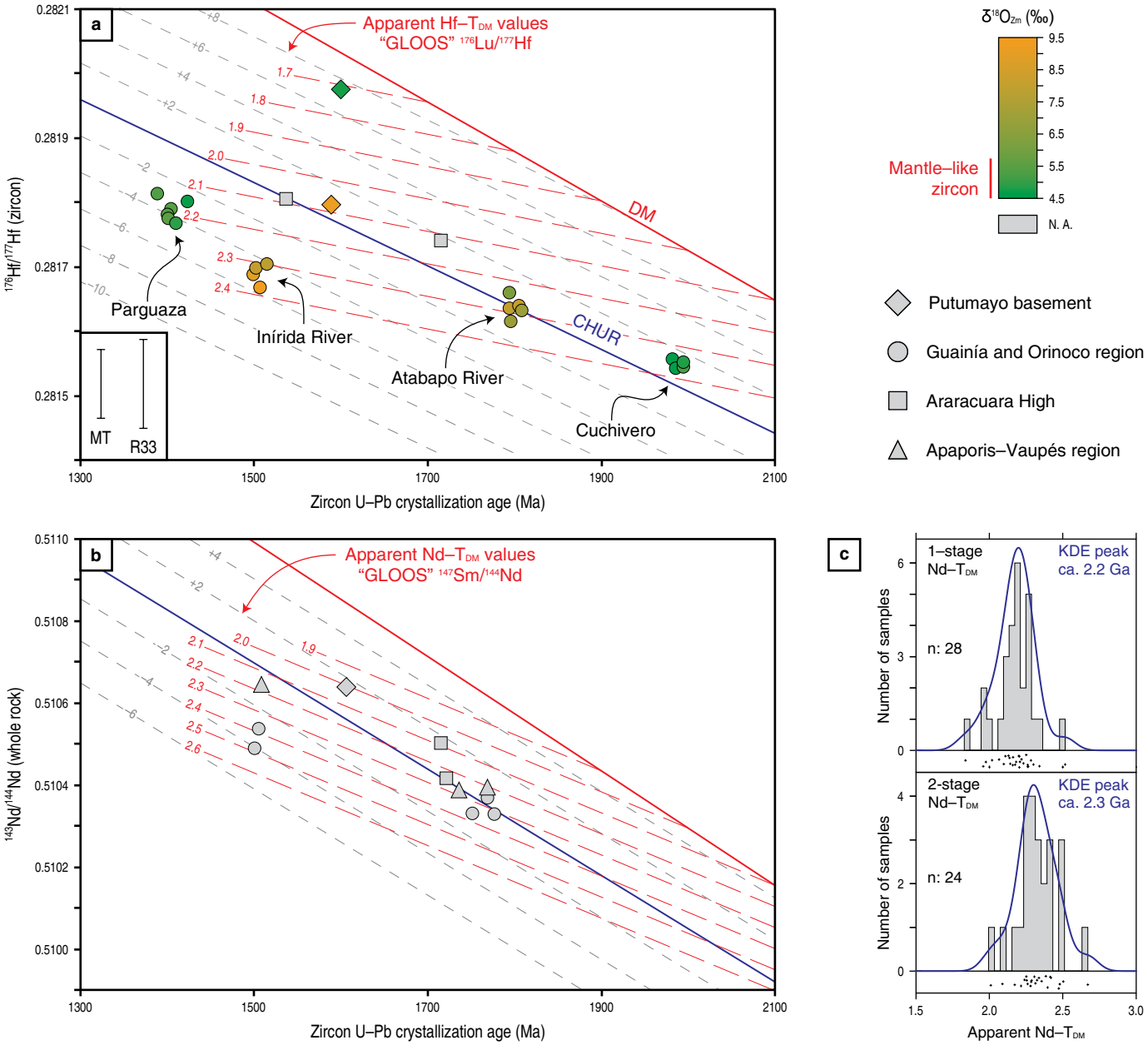

Figure 7. Summary of all available Lu–Hf and Sm–Nd isotopic data for the basement of the western Guiana Shield, corrected for radiogenic ingrowth since time of igneous crystallization. **(a)** Initial ^{176}Hf/^{177}Hf values vs. age diagram. Chondritic reference (CHUR) composition is after Bouvier et al. (2008); depleted mantle (DM) model curve is after Vervoort et al. (2017). Apparent iso–T$_{DM}$ (depleted mantle average crustal residence ages) reference lines calculated using a 'GLOOS'–like Lu/Hf composition (^{176}Lu/^{177}Hf = 0.0142; after Plank & Langmuir, 1998) are also shown. Gray dashed line above and below CHUR reflect positive and negative εHf deviations from a chondritic composition, respectively, plotted at +/– 2 ε intervals. δ^{18}O$_{Zrn}$ values (in ‰, relative to VSMOW) are also shown graphically, coded using a green–to–orange gradient (see Table 2 for actual values). **(b)** Initial ^{143}Nd/^{144}Nd values vs. age diagram. Chondritic reference (CHUR) composition is after Bouvier et al. (2008); DM model curve is after DePaolo et al. (1991). Apparent iso–T$_{DM}$ (depleted mantle average crustal residence ages) reference lines calculated using a 'GLOOS'–like Sm/Nd composition (^{147}Sm/^{144}Nd = 0.1349; after Plank & Langmuir, 1998) are also shown. Gray dashed line above and below CHUR reflect positive and negative εNd deviations from a chondritic composition, respectively, plotted at 2 ε intervals. **(c)** Distribution of apparent depleted mantle Nd average crustal residence (Nd–T$_{DM}$) values for all samples analyzed from the western Guiana Shield, calculated using a 1–stage model (upper panel) and a 2–stage model (lower panel). For the 2–stage model, the second stage was calculated using a GLOOS–like Sm/Nd composition for consistency with panel B. Grey histogram reflects the distribution of data using a bin width of 50 my. Blue curve is a Gaussian Kernel Density Distribution (KDE) curve for all data, calculated using *DensityDist* (Pullen et al., 2014) and an optimized bandwidth of 70 my. See main text for details and discussion.

of +7.6 and mantle–like $\delta^{18}O_{Zrn}$ of 5.43 ± 0.23 ‰. Thus, the igneous protolith of the Mandur–2 ortho–amphibolites unambiguously reflect addition of highly radiogenic juvenile material to the Guiana Shield at the end of the Paleoproterozoic; however, all other samples analyzed thus far yield more ambiguous results, reflecting either heterogeneity of mantle sources or evidencing significant contamination with older crustal material at their time of igneous crystallization. The most unradiogenic (i.e., lowest $^{176}Hf/^{177}Hf$) intrusives yet analyzed are those exposed in the Guainía, Vichada, and Orinoco River areas (circles in Figure 7a), indicating that this region is likely underlain by the oldest continental basement. Apparent mean crustal residence (Hf–T_{DM}) values estimated for the Guainía, Vichada, and Orinoco River intrusives range from ca. 2.40 to 2.15 Ga, and exhibit no systematic dependence between mean $\delta^{18}O_{Zrn}$ and apparent Hf–T_{DM} as would be caused by contamination with subducted sediments. The Hf isotopic compositions of two intrusive samples from the Araracuara area are slightly more radiogenic, but still indicative of crustal reworking, yielding εHf_{Zrn} values between 0 and +2 at their time of crystallization and apparent Hf–T_{DM} values ca. 2.1 Ga. The latest Paleoproterozoic (Statherian) basement of the Putumayo Basin displays a more contrasting nature, with one sample clearly indicating older Paleoproterozoic crustal reworking (Payara–1 basement well; $\varepsilon Hf_t \approx 0.8$, $\delta^{18}O_{Zrn} \approx 9.2$), and one sample that reflects addition of unambiguous juvenile material at time of crystallization (Mandur–2 basement well; $\varepsilon Hf_t \approx +7.6$, $\delta^{18}O_{Zrn} \approx 5.43$ ‰).

Although far less common, Sm–Nd whole–rock isotopic data can also be displayed in isotope–ratio vs. age space, where epsilon values can be displayed as positive and negative deviations around the chondritic uniform reservoir (CHUR) composition and iso–T_{DM} contours graphed for any given $^{147}Sm/^{144}Nd$ value (e.g., Ibañez–Mejia et al., 2015). Here, we have plotted the Nd isotopic data in the same manner as the Lu–Hf results for ease of comparison. For the Nd isotopic data in Figure 7b, we have only plotted those samples for which well–determined U–Pb zircon crystallization ages are available from the same material, whereas apparent Nd–T_{DM} histograms (see further discussion below) used all the available Nd isotopic data. Apparent iso–T_{DM} contours for the Nd isotopic data have also been graphed in Figure 6b using the mean $^{147}Sm/^{144}Nd$ isotopic composition of GLOOS (Plank & Langmuir, 1998) as an average of bulk exposed continental crust and to maintain consistency with the interpretations of the Lu–Hf data. The Sm–Nd isotopic results also indicate that the Guainía and Orinoco region samples have the most unradiogenic (lowest $^{143}Nd/^{144}Nd$) initial compositions, which again suggests this area to be underlain by the oldest continental basement; apparent Nd–T_{DM} values for these samples range from ca. 2.25 to 2.50 Ga. Results from the Apaporis–Vaupés as well as the Araracuara regions further SW are again slightly more radiogenic than the Orinoco–Guainía samples on average, but still reflective of older crustal reworking. Apparent Nd–T_{DM} values for the Apaporis, Vaupés, and Araracuara samples are in the range from ca. 2.10 to 2.28 Ga. For the Putumayo Basin basement, Nd results from the Payara–1 well are also in line with the Hf results discussed above, as they indicate a Nd–T_{DM} value near 2.01 Ga and thus also highlight the presence of Paleoproterozoic basement in this region.

Another way to illustrate the Nd isotopic data is by calculating the apparent Nd–T_{DM} values (using 1– or 2–stage calculations) of samples with known $^{147}Sm/^{144}Nd_0$ and $^{143}Nd/^{144}Nd_0$, even if U–Pb crystallization ages for the same material are not available. This comparison is shown in Figure 7c, where 1–stage Nd–T_{DM} values are calculated by extrapolating the samples' isotopic composition up to the depleted mantle (DM) curve using their known $^{147}Sm/^{144}Nd_0$, and 2–stage values are calculated by using the samples' $^{147}Sm/^{144}Nd_0$ value only up to their known (or an inferred) crystallization age, and a second stage following an empirically determined $^{147}Sm/^{144}Nd$ slope (DePaolo et al., 1991). In both cases, the DM curve assumed for these calculations used the parameters of DePaolo et al. (1991), while the 2–stage model assumed a GLOOS–like $^{147}Sm/^{144}Nd$ composition for the second stage to keep results consistent with those shown in Figure 7b. Once a discrete distribution of apparent Nd–T_{DM} values is calculated using both approaches (frequency histograms in Figure 7c), a continuous probability curve can be approximated using a kernel density estimate (KDE) such that no assumptions need to be made about the uncertainty of each individual Nd–T_{DM} determination; using this approach, the 'smoothing' Kernel bandwidth is only a function of the local density of data. The KDE curves shown in Figure 7c (blue curves) were calculated using the *DensityDist* code of Pullen et al. (2014), which incorporates optimal bandwidth estimations based on the local density of points in the distribution using the algorithms of Botev et al. (2010). Using the 1–stage Nd–T_{DM} approach, KDE calculations show a maximum located at ca. 2.2 Ga, whereas 2–stage calculations display a maximum centered at ca. 2.3 Ga. By combining all available Nd isotopic data, these results indicate what the most likely value of mean residence age is for the crustal material exposed in the region. Considering the likelihood of Sm/Nd partitioning during older crustal reworking, the 2–stage calculations are considered to more closely approximate the time of mean crustal residence. Thus, the Nd data indicates that while apparent individual T_{DM} values in eastern Colombia range from ca. 2.1 to 2.4 Ga in magnitude, the most–likely value of mean crustal residence is ca. 2.3 Ga (lower panel in Figure 7c).

In summary, Lu–Hf and Sm–Nd isotopic results clearly indicate that the late–Paleo– through mid–Mesoproterozoic basement of eastern Colombia is not as radiogenic as global 'depleted mantle' models would predict for a typical juvenile terrane; however, there is no single interpretation for this observation, and we suggest that this could either reflect: (i) Derivation from heterogeneous mantle sources, which might have

been affected by previous metasomatic episodes or simply not be as depleted as global MORB–based DM models suggest, or (ii) that these magmas incorporated a significant proportion of older crustal material of at least Rhyacian and potentially as old as Neoarchean age. These observations seem somewhat at odds with a simple model explaining the growth of the Amazonian Craton in this area by lateral juvenile–arc accretion, but instead suggest that crustal development was a protracted process resulting from a combination of juvenile additions and older crustal reworking. Such observations can be the end result of alternating extensional and compressional accretionary tectonics outboard a continental margin, such as has been described for the Tasmanide margin of eastern Australia (e.g., Kemp et al., 2009) and also recently for the Yavapai–Masatzal Province of Laurentia (Holland et al., 2018).

3.4. The Proterozoic of the Westernmost Guiana Shield within the Context of the Amazonian Craton

The most accepted models for the crustal evolution of the Amazonian Craton involve progressive growth by lateral accretion of Paleo– and Mesoproterozoic arc terranes onto an older Archean nucleus (e.g., Cordani & Teixeira, 2007; Tassinari & Macambira, 1999). These models describe growth as proceeding from northeast to southwest (in modern coordinates), and thus predict that crystallization ages as well as mean crustal residence values in the Guiana and Guaporé Shields should decrease towards the Andean margin of South America (Figure 1). Cordani & Teixeira (2007) proposed the limit between the mid Paleoproterozoic Ventuari–Tapajós Province (VTP) and mid Paleo– to early–Mesoproterozoic Rio Negro–Juruena Province (RNJP) in Colombia to be located near Puerto Inírida, whereas the limit between RNJP and the Rondonian–San Ignacio Province (RSIP) would project just west of Mitú (as shown in Figure 2). These hypotheses are now testable using the recent geochronologic and isotopic dataset as compiled here.

Although on a broad sense the igneous crystallization ages obtained thus far for the western Guiana Shield basement (Figure 6) are in good general agreement with existing models for the evolution of the Amazonian Craton, the new data also reveal important differences with respect to these models that are worth highlighting. For instance, as previously pointed out by Ibañez–Mejia et al. (2011, 2015), the Rondonian–San Ignacio Province appears to be absent or at least poorly represented in Colombia, as no collision–related 1.55 to 1.30 Ga tectonothermal events have been identified in the exposed craton or in the basement of the Putumayo Basin. In addition, more recently Cordani et al. (2016b) interpreted both the 'Atabapo Belt' and the 'Vaupés Belt' as belonging to the RNJP, an interpretation which implies that: (i) The RNJP–RSIP boundary is not present in Colombia just west of Mitú (or possibly even at all) as previously thought, and (ii) the areal extent of mid–Paleo– to early–Mesoproterozoic Rio Negro–Juruena–like basement domains in Colombia and the W Guiana Shield is significantly larger than previously expected.

On the other hand, the U–Pb data confirm that the expected age transition for the VTP–RNJP boundary near the Colombian–Venezuelan border is in fact present. Although previous models suggested this boundary to be west of Puerto Inírida, the new data from the Colombia–Venezuela border suggest its potential location might in fact be farther east, at least along the Atabapo River (as suggested by Cordani et al., 2016b and shown in Figure 2) or possibly to the east of the Ventuari River. Lastly, although it still remains unclear whether two distinct ca. 1.80 and ca. 1.55 Ga orogenic belts can be clearly discerned in eastern Colombia, the U–Pb data is unequivocal at pointing out the relevance of these two major magmatic episodes in shaping the Proterozoic basement of the region as interpreted by Cordani et al. (2016b).

From a crustal–growth perspective, the Hf and Nd data of Figure 7 reveal the general lack of highly radiogenic mid– to late–Paleoproterozoic crust in the region. The moderately positive to negative εHf and εNd values at time of crystallization obtained from almost all mid Paleo– to early–Mesoproterozoic intrusives in the westernmost Guiana Shield, indicate the widespread incorporation of some proportion of reworked older crustal material. Based on the apparent Hf– and Nd–T_{DM} values of samples calculated using GLOOS–like Lu/Hf and Sm/Nd compositions (Figure 7a, 7b), or the alignment of geographically associated samples in $^{176}Hf/^{177}Hf$ vs. U–Pb age space (Ibañez–Mejia, 2014), the age of the reworked crustal contaminants may range from Rhyacian to Neoarchean in age. Because accretionary belts could be the result of complex juxtaposition of tectonic units, including a great deal of intra–oceanic material with positive or slightly negative $\varepsilon Nd_{(t)}$ signatures, but also containing in places cordilleran–type granites, collisional–type belts, microcontinents, volcano–sedimentary basins, and post–tectonic to anorogenic–type complexes, we emphasize that the incorporation of older crustal material identified in the basement of eastern Colombia does not necessarily stand at odds with an accretionary tectonic model.

Mantle–derived material of "intra–oceanic" origin is difficult to be characterized solely by isotopic geochemistry. The use of $\varepsilon Nd_{(t)}$ or $\varepsilon Hf_{(t)}$ to trace juvenile processes is not completely unequivocal, because mantle sources (e.g., deep mantle material exhumed by plumes, mantle affected by metasomatism, or lithospheric mantle enriched by earlier recycling of crustal material) display varying ranges of 'depletion'. In most papers published in the last 30 years (many co–authored by Cordani), the Rio Negro–Juruena Province has been characterized as composed predominantly of granitoid rocks, deformed or not, yielding slightly positive to slightly negative $\varepsilon Nd_{(t)}$ signatures (roughly between +4.0 and –2.0);

this information has been used to suggest that juvenile accretionary events played a major role in its tectonic evolution. All samples from eastern Colombia analyzed thus far for Sm–Nd yield Paleoproterozoic Nd–T_{DM} values roughly between 1.9 and 2.5 Ga, regardless of their U–Pb zircon ages (Figure 7c; Table 2; Cordani et al. 2016b), thus suggesting the absence of a much older (Archean?) source material. Moreover, given that the $\varepsilon Nd_{(t)}$ values of the granitoid rocks are near zero or slightly positive or negative, the presence of juvenile material may have been important, and at least part of the magmatic arcs in the NW corner of the Rio Negro–Juruena Province could have been intra–oceanic. This interpretation is what is included in the Tectonic Map of South America. However, although the isotopic results shown in Figure 6 do not unequivocally show the presence of Archean crust in the region, the isotopic results in Colombia and western Venezuela seem to indicate a greater degree of older Paleoproterozoic reworking in the western Guiana Shield relative to correlative magmatic domains exposed south of the Amazon Basin.

3.5. Cretaceous Tectonic Reactivation and Thermal Effects in the Colombian Continental Interior

The recent discovery that Cretaceous mafic magmatism affected the basement of the Araracuara High (Ibañez–Mejia, 2014), expands the known extent of Mesozoic magmatic activity far beyond the easternmost locus of Cretaceous mafic intrusives known along the Eastern Cordillera axis (e.g., Vasquez et al., 2010). A dolerite dike intruding the Araracuara Gneiss yielded an age of 102.5 ± 2.2/2.3 Ma (Ibañez–Mejia, 2014) indicating that, during the Albian, this area was likely undergoing active extension and heating, synchronous to similar events occurring along the Eastern Cordillera. These results are important for two main reasons: (i) They suggest that Güejar–Apaporis Graben–related structures (Figure 2) were likely reactivated as intra–continental extensional domains during the mid–Cretaceous, coeval with extension, sedimentation, and mafic magmatism occurring along the Eastern Cordillera (e.g., Mora et al., 2009; Vasquez et al., 2010); and (ii) the age of this dolerite intrusion constrains the timing of uplift of the serranía de Chiribiquete and ultimate exhumation of the Araracuara Formation to post–Albian times, which is of importance for understanding the landscape evolution of the Colombian Amazon as well as the sedimentation history of the Late Cretaceous and Cenozoic basins of the Eastern Cordillera and its foreland (e.g., Horton et al., 2010). Although clearly outside the main scope of this chapter, we highlight the importance of this observation to argue that future efforts should be aimed at better resolving the structural as well as the temporal history of Cretaceous heating and tectonic re–activation in the eastern Colombian basement.

3.6. Future Challenges and Outstanding Questions in Colombian Precambrian Geology

This chapter presents an attempt to summarize and highlight the new advances in our understanding of the Precambrian geology of eastern Colombia, and the westernmost Guiana Shield in general. However, it should be realized that this vast area still remains one of the least explored regions in the South American continent, and thus many of the interpretations provided here are likely to be refined and modified as the geochronologic and other isotopic datasets continue to expand. Although by no means a comprehensive list, some of the main questions and/or future challenges the community needs to be address to better understand the basement in this area are:

a. We need to move past outdated stratigraphic nomenclature, and develop a local (tectono)–stratigraphic framework that is in line with modern petrologic and tectonic concepts, as well as recent geochronologic data. Although we make no attempts to propose formal modifications here, we particularly urge the community to think beyond (and ultimately abandon) the term Mitú Migmatitic Complex, to focus on developing a more accurate and detailed stratigraphic nomenclature.

b. The "granitoid basement" that cover the entire western half of the Guiana Shield remains poorly known, because geological mapping and geochemical/geochronological research has not yet progressed to a stage that would allow for a better characterization. We know that the entire region is formed by granitoid rocks (sensu lato), but it is not possible, at present, to make a clear distinction between syn–, late–, and post–tectonic, or anorogenic granitoid intrusions of various types and ages. Large parts of this province are poorly controlled by U–Pb dates and Nd–Hf isotopic constraints. More of this robust radioisotopic data, such as that compiled in this chapter, are needed.

c. The presence/absence and location of major terrane boundaries in the basement of eastern Colombia is critical for accurately placing this portion of the Guiana Shield within a larger tectonic framework. For instance, these boundaries are critical for better establishing potential correlations with the Central Brazilian Shield within the concept of a unified 'Amazonian Craton' (e.g., Cordani & Teixeira, 2007; Tassinari & Macambira, 1999), and also for evaluating the continuity of these domains to other cratons under the light of potential Columbia/Nuna and Rodinia paleogeographic configurations (e.g., Bispo–Santos et al., 2014a, 2014b; Cawood & Pisarevski, 2017; Cordani et al., 2009; D'Agrella–Filho et al., 2016; Ibañez–Mejia et al., 2011; Johansson, 2009; Li et al., 2008; Pisarevsky et al., 2014; Santos et al., 2008, among many others). The geochronologic data in this region has so far failed to identify the presence of a Rondonian–San Ignacio–like province

as defined in NW Brasil and Bolivia (Bettencourt et al., 2010), but further efforts to confirm and/or negate this conclusion, as well as continue to evaluate other potential cratonic boundaries, are still necessary.

d. The combination of U–Pb, Lu–Hf and $\delta^{18}O$ isotopic information in zircon is a powerful tool to disentangle complex tectonic histories as well as revealing the mechanisms driving crustal maturation and evolution (e.g., Ibañez–Mejia, 2014; Ibañez–Mejia et al., 2015; Iizuka et al., 2017; Kemp et al., 2009; Valley et al., 2005; Vervoort & Kemp, 2016, among others). Further studies aiming to produce combined U–Pb–Hf–O datasets in zircons from the Guiana Shield offer the best path forward to resolve many of the outstanding issues of the tectonic evolution of the region.

e. There is a general dearth of geochronologic and isotopic data from mafic magmatic units in eastern Colombia and the Guiana Shield. Mafic magmatic events, in particular dike swarms potentially associated with Large Igneous Provinces (LIPs), have become a critical piece in the Precambrian tectonic puzzle. This is primordially due to their utility for providing geologic 'piercing points' amongst cratonic regions (Ernst et al., 2013) as well as acting as robust carriers of paleomagnetic information (e.g., Evans, 2013; Li et al., 2008; Pisarevsky et al., 2014). In the absence of zircon, mafic rocks can now be routinely and accurately dated using baddeleyite U–Pb geochronology by ID–TIMS (e.g., Söderlund et al., 2010), secondary ion mass spectrometry (SIMS; e.g., Chamberlain et al., 2010; Schmitt et al., 2010), or LA–ICP–MS (Ibañez–Mejia et al., 2014), and the latter approach also provides an opportunity to obtain Lu–Hf isotopic data. Future studies aimed at better understanding the mafic magmatic 'barcode' of the Guiana Shield (e.g., Reis et al., 2013; Teixeira et al., 2015) will surely bring significant advances for understanding the geology of the region and more accurately placing it within a global paleo–tectonic framework.

4. Conclusions

The U–Pb geochronologic data available for the westernmost Guiana Shield demonstrates that the basement of eastern Colombia and neighboring regions in Venezuela and Brasil is dominantly Paleo– and Mesoproterozoic in age, crystallized between ca. 1.99 and 1.38 Ga. The distribution of crystallization ages in not continuous, but rather clusters into four main periods that reflect major episodes of magmatic activity throughout the region. These are: (i) A mid–Paleoproterozoic event ca. 1.99 Ga, responsible for the development of the Cuchivero magmatic belt in Venezuela; (ii) a mid– to late–Paleoproterozoic event ranging from 1.84 to 1.72 Ga, preliminarily referred to here as the 'Atabapo Belt'; (iii) an early–Mesoproterozoic event ranging from 1.59 to 1.50 Ga, preliminarily referred to here as the 'Vaupés Belt'; and (iv) a mid–Mesoproterozoic event from 1.42 to 1.39 Ga, associated with the emplacement of the Parguaza anorogenic massif along the Colombia–Venezuela border. The combined Nd, Hf, and O isotopic systematics of granitoids in the area reveal the absence of highly radiogenic material associated with these magmatic pulses, suggesting that either: (i) The sub–continental mantle underlying the westernmost Guiana Shield was highly heterogeneous and less radiogenic than global mantle models would suggest, and/or (ii) that this basement is the result of combined juvenile additions with pervasive reworking of older crust of possible early Paleoproterozoic to late Neoarchean age.

Based on the diversity of ages, lithologies, and processes involved in shaping the geology of the eastern Colombia basement, we consider the definition of the Mitú Migmatitic Complex' to be inadequate moving forward, and urge the community to develop a more accurate and detailed nomenclature that is in line with recent geochronologic, isotopic, and petrologic research in this area.

The U–Pb and Nd isotopic result from a dolerite dike in the Araracuara area indicate that not all the magmatic activity in eastern Colombia is Precambrian in age, but reveal that Cretaceous mafic magmatism was in part responsible for controlling the geologic evolution of the area. Future studies aimed at better resolving the timing and nature of mafic magmatism in the region will thus be crucial for understanding the structural, thermal, as well as the landscape evolution of the eastern Colombian lowlands.

These are exciting times for the geology of the western Guiana Shield (!), as the development of new analytical tools for spatially–resolved geochronologic and geochemical analyses of zircon and baddeleyite now allow interrogating the geologic evolution of this complex region in greater detail than was ever possible before. We hope that the observations and ideas outlined in this chapter will serve as the launching pad for many exciting advances in understanding the geology of the western Guiana Shield in years and decades to come.

Acknowledgements

The authors would like to thank the Servicio Geologico Colombiano, particularly Jorge GÓMEZ TAPIAS and Oscar PAREDES ZAPATA for their invitation to contribute a chapter to this book. MI specially acknowledges the Guacamayo community in Araracuara, especially the Macuritofe family for their support during fieldwork, and the support that Franco URBANI, David MENDI, Zeze AMAYA, and Felipe VILLEGAS provided during various trips to the Guiana Shield in Venezuela and Colombia. UGC wishes to thank the Servicio Geologico Colombiano for the provision of samples collected during the PRORADAM. He also acknowledges the Fundação de Amparo à Pesquisa do estado de Sao Paulo for the allocation of a grant (Project 2013/12754–0) that made

possible the acquisition of the geochronological analyses made on the Colombian samples. Reviewers Leda M. FRAGA and Salomon KROONENBERG are thanked for their thoughtful and in–depth comments that helped improve the final version of this chapter. Support for writing this chapter was provided to MI by the University of Rochester.

References

Aldrich, L.T., Herzog, L.F., Doak, J.B. & Davis, G.L. 1953. Variations in strontium isotope abundances in minerals part I: Mass spectrometry analysis of mineral sources of strontium. Eos, Transactions American Geophysical Union, 34(3): 457–460. https://doi.org/10.1029/TR034i003p00457

Almeida, M.E., Macambira, M.J.B., Santos, J.O.S., do Nascimento, R.S.C. & Paquette, J.L. 2013. Evolução crustal do noroeste do Cráton Amazônico, Amazonas, Brasil, baseada em dados de campo, geoquímicos e geocronológicos. 13° Simpósio de Geologia da Amazônia, Anais, p. 201–204. Belém, Brazil.

Barrera, J.I. 1988. Contribución al conocimiento y petrografía del Complejo Migmatítico de Mitú y su correlación en las localidades de Araracuara y alrededores. Bachelor thesis, Universidad Nacional de Colombia, 123 p. Bogotá.

Barrios, F.J. 1983. Caracterização geocronológica da região amazônica da Venezuela. Master thesis, Universidade de São Paulo, 123 p. Sao Paulo, Brasil. https://doi.org/10.11606/D.44.1983.tde-15072015-155335

Barrios, F., Rivas, D., Cordani, U. & Kawashita, K. 1985. Geocronología del territorio federal Amazonas. I Simposium Amazónico, Memoirs, Boletín de Geología, Publicación Especial 10: 22–31. Puerto Ayacucho, Venezuela.

Barrios, F., Cordani, U.G. & Kawashita, K. 1986. Caracterización geocronologica del territorio federal Amazonas, Venezuela. VI Congreso Geológico Venezolano, Memoirs III, p. 1432–1480. Caracas, Venezuela.

Bettencourt, J.S., Leite, Jr., W.B., Ruiz, A.S., Matos, R., Payolla, B.L. & Tosdal, R.M. 2010. The Rondonian–San Ignacio Province in the SW Amazonian Craton: An overview. Journal of South American Earth Sciences, 29(1): 28–46. http://doi.org/10.1016/j.jsames.2009.08.006

Bispo–Santos, F., D'Agrella–Filho, M.S., Trindade, R.I.F., Janikian, L. & Reis, N.J. 2014a. Was there SAMBA in Columbia? Paleomagnetic evidence from 1790 Ma Avanavero mafic sills, northern Amazonian Craton. Precambrian Research, 244: 139–155. http://doi.org/10.1016/j.precamres.2013.11.002

Bispo–Santos, F., D'Agrella–Filho, M.S., Janikian, L., Reis, N.J., Trindade, R.I.F. & Reis, M.A.A.A. 2014b. Towards Columbia: Paleomagnetism of 1980–1960 Ma Surumu volcanic rocks, northern Amazonian Craton. Precambrian Research, 244: 123–138. http://doi.org/10.1016/j.precamres.2013.08.005

Bonilla–Pérez, A., Frantz, J.C., Charão–Marques, J., Cramer, T., Franco–Victoria, J.A., Mulocher, E. & Amaya–Perea, Z. 2013. Petrografía, geoquímica y geocronología del Granito de Parguaza en Colombia. Boletín de Geología, 35(2): 83–104.

Botev, Z.I., Grotowski, J.F. & Kroese, D.P. 2010. Kernel density estimation via diffusion. The Annals of Statistics, 38(5): 2916–2957. http://doi.org/10.1214/10-AOS799

Bouvier, A., Vervoort, J.D. & Patchett, P.J. 2008. The Lu–Hf and Sm–Nd isotopic composition of CHUR: Constraints from unequilibrated chondrites and implications for the bulk composition of terrestrial planets. Earth and Planetary Science Letters, 273(1–2): 48–57. http://doi.org/10.1016/j.epsl.2008.06.010

Carneiro, M.C.R., Nascimento, R.S.C., Almeida, M.E., Salazar, C.A., da Trindade, I.R., de Oliveira–Rodrigues, V. & Passos, M.S. 2017. The Cauaburi magmatic arc: Litho–stratigraphic review and evolution of the Imeri Domain, Rio Negro Province, Amazonian Craton. Journal of South American Earth Sciences, 77: 310–326. http://doi.org/10.1016/j.jsames.2017.06.001

Cawood, P.A. & Pisarevsky, S.A. 2017. Laurentia–Baltica–Amazonia relations during Rodinia assembly. Precambrian Research, 292: 386–397. http://doi.org/10.1016/j.precamres.2017.01.031

Celada, C.M., Garzón, M., Gómez, E., Khurama, S., López, J.A., Mora, M., Navas, O., Pérez, R., Vargas, O. & Westerhof, A.B. 2006. Potencial de recursos minerales en el oriente colombiano: Compilación y análisis de la información geológica disponible (fase 0). Servicio Geológico Colombiano, unpublished report, 165 p. Bogotá.

Chamberlain, K.R., Schmitt, A.K., Swapp, S.M., Harrison, T.M., Swoboda–Colberg, N., Bleeker, W., Peterson, T.D., Jefferson, C.W. & Khudoley, A.K. 2010. In situ U–Pb SIMS (IN–SIMS) micro–baddeleyite dating of mafic rocks: Method with examples. Precambrian Research, 183(3): 379–387. http://doi.org/10.1016/j.precamres.2010.05.004

Cordani, U.G. & Teixeira, W. 2007. Proterozoic accretionary belts in the Amazonian Craton. In: Hatcher Jr, R.D., Carlson, M.P., McBride, J.H. & Martínez–Catalá, J.R. (editors), 4–D Framework of continental crust. Geological Society of America, Memoir 200, p. 297–320. https://doi.org/10.1130/2007.1200(14)

Cordani, U.G., Tassinari, C.C.G., Teixeira, W., Basei, M.A.S. & Kawashita, K. 1979. Evolução tectônica da Amazônia com base nos dados geocronológicos. II Congreso Geológico Chileno, Memoirs 4, p. 137–148. Arica, Chile.

Cordani, U.G., Teixeira, W., D'agrella–Filho, M.S. & Trindade, R.I. 2009. The position of the Amazonian Craton in supercontinents. Gondwana Research, 15(3–4): 396–407. http://doi.org/10.1016/j.gr.2008.12.005

Cordani, U.G., Ramos, V.A., Fraga, L.M., Delgado, I., de Souza, K.G., Gomes, F.E.M., Schobbenhaus, C. & Cegarra, M. 2016a. Tectonic map of South America, 2nd edition. Scale 1:5 000 000. Commission for the Geological Map of the World.

Cordani, U.G., Sato, K., Sproessner, W. & Fernandes, F.S. 2016b. U–Pb zircon ages of rocks from the Amazonas territory of Colombia and their bearing on the tectonic history of the NW sector

of the Amazonian Craton. Brazilian Journal of Geology, 46(1): 5–35. http://doi.org/10.1590/2317-4889201620150012

D'Agrella–Filho, M.S., Trindade, R.I.F., Queiroz, M.V.B., Meira, V.T., Janikian, L., Ruiz, A.S. & Bispo–Santos, F. 2016. Reassessment of Aguapeí, Salto do Céu, paleomagnetic pole, Amazonian Craton and implications for Proterozoic supercontinents. Precambrian Research, 272: 1–17. http://doi.org/10.1016/j.precamres.2015.10.021

DePaolo, D.J., Linn, A.M. & Schubert, G. 1991. The continental crustal age distribution: Methods of determining mantle separation ages from Sm–Nd isotopic data and application to the southwestern United States. Journal of Geophysical Research: Solid Earth, 96(B2): 2071–2088. https://doi.org/10.1029/90JB02219

Ernst, R.E., Bleeker, W., Soderlund, U. & Kerr, A.C. 2013. Large Igneous Provinces and supercontinents: Toward completing the plate tectonic revolution. Lithos, 174: 1–14. http://doi.org/10.1016/j.lithos.2013.02.017

Evans, D.A.D. 2013. Reconstructing pre–Pangean supercontinents. Geological Society of America Bulletin, 125(11–12): 1735–1751. http://doi.org/10.1130/B30950.1

Fernandes, P.E.C.A., Pinheiro, S. da S., de Montalvão, R.M.G., Issler, R.S., Abreu, A.S. & Tassinari, C.C.G. 1976. Geologia. In: Divisão de publicação (editor), Projeto RADAMBRASIL. Levantamento de recursos naturais: Folha SA. 19 Içá, 11, p. 17–123. Rio de Janeiro, Brazil.

Fuck, R.A., Brito–Neves, B.B. & Schobbenhaus, C. 2008. Rodinia descendants in South America. Precambrian Research, 160(1–2): 108–126. http://doi.org/10.1016/j.precamres.2007.04.018

Galvis, J., Huguett, A. & Ruge, P. 1979. Geología de la Amazonia colombiana. Boletín Geológico, 22(3): 3–86.

Gaudette, H.E. & Olszewski Jr., W.J. 1985. Geochronology of the basement rocks, Amazonas territory, Venezuela and the tectonic evolution of the western Guiana Shield. Geologie en Mijnbouw, 64(2): 131–143.

Gaudette, H.E., Mendoza, V., Hurley, P.M. & Fairbairn, H.W. 1978. Geology and age of the Parguaza rapakivi granite, Venezuela. Geological Society of America Bulletin, 89(9): 1335–1340. https://doi.org/10.1130/0016-7606(1978)89<1335:GAAOTP>2.0.CO;2

Gibbs, A.K. 1987. Proterozoic volcanic rocks of the northern Guiana Shield, South America. In: Pharaoh, T.C., Beckinsale, R.D. & Rickard, D. (editors), Geochemistry and mineralization of Proterozoic volcanic suites. Geological Society of London, Special Publication 33, p. 275–288. London. https://doi.org/10.1144/GSL.SP.1987.033.01.19

Gibbs, A.K. & Barron, C.N. 1993. Geology of the Guiana Shield. Claredon Press, 245 p. New York, USA.

Gómez, J., Montes, N.E., Almanza, M.F., Alcárcel, F.A., Madrid, C.A. & Diederix, H. 2017. Geological map of Colombia 2015. Episodes, 40(3): 201–212. https://doi.org/10.18814/epiiugs/2017/v40i3/017023

Hawkesworth, C.J., Dhuime, B., Pietranik, A.B., Cawood, P.A., Kemp, A.I.S. & Storey, C.D. 2010. The generation and evolution of the continental crust. Journal of the Geological Society, 167(2): 229–248. http://doi.org/10.1144/0016-76492009-072

Herzog, L.F. 1952. Natural variations in strontium isotope abundances in minerals: A possible geologic age method. Doctoral thesis, Massachusetts Institute of Technology, 122 p. Cambridge, USA.

Holland, M.E., Karlstrom, K.E., Gehrels, G.E., Shufeldt, O.P., Begg, G., Griffin, W. & Belousova, E. 2018. The Paleoproterozoic Vishnu Basin in southwestern Laurentia: Implications for supercontinent reconstructions, crustal growth, and the origin of the Mojave crustal province. Precambrian Research, 308: 1–17. https://doi.org/10.1016/j.precamres.2018.02.001

Horton, B.K., Saylor, J.E., Nie, J., Mora, A., Parra, M., Reyes–Harker, A. & Stockli, D.F. 2010. Linking sedimentation in the northern Andes to basement configuration, Mesozoic extension, and Cenozoic shortening: Evidence from detrital zircon U–Pb ages, Eastern Cordillera, Colombia. Geological Society of America Bulletin, 122(9–10): 1423–1442. http://doi.org/10.1130/B30118.1

Ibañez–Mejia, M. 2014. Timing and rates of Precambrian crustal genesis and deformation in northern South America. Doctoral thesis, University of Arizona, 334 p. Tucson, USA.

Ibañez–Mejia, M. 2020. The Putumayo Orogen of Amazonia: A synthesis. In: Gómez, J. & Mateus–Zabala, D. (editors), The Geology of Colombia, Volume 1 Proterozoic – Paleozoic. Servicio Geológico Colombiano, Publicaciones Geológicas Especiales 35, p. 101–131. Bogotá. https://doi.org/10.32685/pub.esp.35.2019.06

Ibañez–Mejia, M., Ruiz, J., Valencia, V.A., Cardona, A., Gehrels, G.E. & Mora, A.R. 2011. The Putumayo Orogen of Amazonia and its implications for Rodinia reconstructions: New U–Pb geochronological insights into the Proterozoic tectonic evolution of northwestern South America. Precambrian Research, 191(1–2): 58–77. https://doi.org/10.1016/j.precamres.2011.09.005

Ibañez–Mejia, M., Gehrels, G.E., Ruiz, J., Vervoort, J.D., Eddy, M.E. & Li, C. 2014. Small–volume baddeleyite (ZrO_2) U–Pb geochronology and Lu–Hf isotope geochemistry by LA–ICP–MS. Techniques and applications. Chemical Geology, 384: 149–167. http://doi.org/10.1016/j.chemgeo.2014.07.011

Ibañez–Mejia, M., Pullen, A., Arenstein, J., Gehrels, G.E., Valley, J., Ducea, M.N., Mora, A.R., Pecha, M. & Ruiz, J. 2015. Unraveling crustal growth and reworking processes in complex zircons from orogenic lower–crust: The Proterozoic Putumayo Orogen of Amazonia. Precambrian Research, 267: 285–310. http://doi.org/10.1016/j.precamres.2015.06.014

Iizuka, T., Yamaguchi, T., Itano, K., Hibiya, Y. & Suzuki, K. 2017. What Hf isotopes in zircon tell us about crust–mantle evolution. Lithos, 274–275: 304–327. http://doi.org/10.1016/j.lithos.2017.01.006

Johansson, A. 2009. Baltica, Amazonia and the SAMBA connection–1000 million years of neighborhood during the Proterozoic? Precambrian Research, 175(1–4): 221–234. http://doi.org/10.1016/j.precamres.2009.09.011

Kemp, A.I.S., Hawkesworth, C.J., Collins, W.J., Gray, C.M., Blevin, P.L. & Edinburgh Ion Microprobe Facility. 2009. Isotopic evidence for rapid continental growth in an extensional accretionary orogen: The Tasmanides, eastern Australia. Earth and Planetary Science Letters, 284(3–4): 455–466. http://doi.org/10.1016/j.epsl.2009.05.011

Kronenberg, S. & Reeves, C.V. 2011. Vaupés and Amazonas Basins. In: Cediel, F. (editor), Petroleum geology of Colombia: Geology and hydrocarbon potential, 15. Agencia Nacional de Hidrocarburos and Universidad EAFIT, 103 p. Medellín.

Li, Z.X., Bogdanova, S.V., Collins, A.S., Davidson, A., de Waele, B., Ernst, R.E., Fitzsimons, I.C.W., Fuck, R.A., Gladkochub, D.P. Jacobs, J., Karlstrom, K.E., Lu, S., Natapov, L.M., Pease, V., Pisarevsky, S.A., Thrane, K. & Vernikovsky, V. 2008. Assembly, configuration, and break–up history of Rodinia: A synthesis. Precambrian Research, 160(1–2): 179–210. http://doi.org/10.1016/j.precamres.2007.04.021

Lugmair, G. W. & Marti, K. 1978. Lunar initial $^{143}Nd/^{144}Nd$: Differential evolution of the lunar crust and mantle. Earth and Planetary Science Letters, 39(3): 349–357. http://doi.org/10.1016/0012-821X(78)90021-3

Mora, A., Gaona, T., Kley, J., Montoya, D., Parra, M., Quiroz, L.I., Reyes, G. & Strecker, M. 2009. The role of inherited extensional fault segmentation and linkage in contractional orogenesis: A reconstruction of Lower Cretaceous inverted rift basins in the Eastern Cordillera of Colombia. Basin Research, 21(1): 111–137. https://doi.org/10.1111/j.1365-2117.2008.00367.x

Nier, A.O. 1940. A Mass spectrometer for routine isotope abundance measurements. Review of Scientific Instruments, 11(7): 212–216. http://doi.org/10.1063/1.1751688

Nier, A.O. 1947. A mass spectrometer for isotope and gas analysis. Review of Scientific Instruments, 18(6): 398–411. http://doi.org/10.1063/1.1740961

Pinheiro, S.S., Fernandes, P.E.C.A., Pereira, E.R., Vasconcelos, E.G., Pinto, A.C., de Montalvão, R.M.G., Issler, R.S., Dall'Agnol, R., Teixeira, W. & Fernandes, C.A.C. 1976. Geologia. In: Divisão de publicação. (editor), Projeto RADAMBRASIL. Levantamento de recursos naturais: Folha NA. 19 Pico da Neblina, 11, p. 19–137. Rio de Janeiro, Brazil.

Pinson Jr, W.H., Hurley, P.M., Mencher, E. & Fairbairn, H.W. 1962. K–Ar and Rb–Sr ages of biotites from Colombia, South America. Geological Society of America Bulletin, 73(7): 907–910. https://doi.org/10.1130/0016-7606(1962)73[907:KARAOB]2.0.CO;2

Pisarevsky, S.A., Elming, S.A., Pesonen, L.J. & Li, Z.X. 2014. Mesoproterozoic paleogeography: Supercontinent and beyond. Precambrian Research, 244: 207–225. http://doi.org/10.1016/j.precamres.2013.05.014

Plank, T. & Langmuir, C.H. 1998. The chemical composition of subducting sediment and its consequences for the crust and mantle. Chemical Geology, 145(3–4): 325–394. http://doi.org/10.1016/S0009-2541(97)00150-2

Priem, H., Andriessen, P., Boelrijk, N., De Booder, H., Hebeda, E., Huguett, A., Verdumen, E. & Verschure, R. 1982. Geochronology of the Precambrian in the Amazonas region of southeastern Colombia (western Guiana Shield). Geologie en Mijnbouw, 61(3): 229–242.

Pullen, A., Ibañez–Mejia, M., Gehrels, G.E., Ibañez–Mejia, J.C. & Pecha, M. 2014. What happens when n=1000? Creating large–n geochronological datasets with LA–ICP–MS for geologic investigations. Journal of Analytical Atomic Spectrometry, 29(6): 971–980. https://doi.org/10.1039/C4JA00024B

Reis, N.J., de Faria, M.S.G., Fraga, L.M. & Haddad, R.C. 2000. Orosirian calc–alkaline volcanism and the Orocaima event in the northern Amazonian Craton, eastern Roraima state, Brazil. Revista Brasileira de Geociencias, 30(3): 380–383.

Reis, N.J., Teixeira, W., Hamilton, M.A., Bispo–Santos, F., Almeida, M.E. & D'Agrella–Filho, M.S. 2013. Avanavero mafic magmatism, a late Paleoproterozoic LIP in the Guiana Shield, Amazonian Craton: U–Pb ID–TIMS baddeleyite, geochemical and paleomagnetic evidence. Lithos, 174: 175–195. http://doi.org/10.1016/j.lithos.2012.10.014

Santos, J.O.S., Hartmann, L.A., Gaudette, H.E., Groves, D.I., McNaughton, N.J. & Fletcher, I.R. 2000. A new understanding of the provinces of the Amazon Craton based on integration of field mapping and U–Pb and Sm–Nd geochronology. Gondwana Research, 3(4): 453–488. https://doi.org/10.1016/S1342-937X(05)70755-3

Santos, J.O.S., Potter, P.E., Reis, N.J., Hartmann, L.A., Fletcher, I.R. & McNaughton, N.J. 2003. Age, source, and regional stratigraphy of the Roraima Supergroup and Roraima–like outliers in northern South America based on U–Pb geochronology. Geological Society of America Bulletin, 115(3): 331–348. https://doi.org/10.1130/0016-7606(2003)115<0331:ASARSO>2.0.CO;2

Santos, J.O.S., Rizzotto, G.J., Potter, P.E., McNaughton, N.J., Matos, R.S., Hartmann, L.A., Cheemale, F. & Quadros, M.E.S. 2008. Age and autochthonous evolution of the Sunsás Orogen in west Amazon Craton based on mapping and U–Pb geochronology. Precambrian Research, 165(3–4): 120–152. http://doi.org/10.1016/j.precamres.2008.06.009

Schmitt, A.K., Chamberlain, K.R., Swapp, S.M. & Harrison, T.M. 2010. In situ U–Pb dating of micro–baddeleyite by secondary ion mass spectrometry. Chemical Geology, 269(3–4): 386–395. http://doi.org/10.1016/j.chemgeo.2009.10.013

Shrock, R.R. 1977. Geology at MIT 1865–1965, 1: The faculty and supporting staff. The MIT press, 1102 p. Cambridge, USA.

Söderlund, U., Patchett, P.J., Vervoort, J. & Isachsen, C.E. 2004. The ^{176}Lu decay constant determined by Lu–Hf and U–Pb isotope systematics of Precambrian mafic intrusions. Earth

and Planetary Science Letters, 219(3–4): 311–324. http://doi.org/10.1016/S0012-821X(04)00012-3

Söderlund, U., Hofmann, A., Klausen, M.B., Olsson, J.R., Ernst, R.E. & Persson, P.O. 2010. Towards a complete magmatic barcode for the Zimbabwe Craton: Baddeleyite U–Pb dating of regional dolerite dyke swarms and sill complexes. Precambrian Research, 183(3): 388–398. http://doi.org/10.1016/j.precamres.2009.11.001

Tassinari, C.C.G. & Macambira, M.J.B. 1999. Geochronological provinces of the Amazonian Craton. Episodes, 22(3): 174–182.

Tassinari, C.C.G., Cordani, U.G., Nutman, A.P., van Schmus, W.R., Bettencourt, J.S. & Taylor, P.N. 1996. Geochronological systematics on basement rocks from the Rio Negro–Juruena Province, Amazonian Craton, and tectonic implications. International Geology Review, 38(2): 161–175. https://doi.org/10.1080/00206819709465329

Teixeira, W., Tassinari, C.C.G. & Mondin, M. 2002. Características isotópicas (Nd e Sr) do plutonismo intrusivo no extremo NW do Cráton Amazônico, Venezuela, e implicações para a evolução Paleoproterozóica. Revista do Instituto de Geociências da Universidade de Sao Paulo, 2(1): 131–141. https://doi.org/10.5327/S1519-874X2002000100011

Teixeira, W., Hamilton, M.A., Lima, G.A., Ruiz, A.S., Matos, R. & Ernst, R.E. 2015. Precise ID–TIMS U–Pb baddeleyite ages (1110–1112 Ma) for the Rincón del Tigre–Huanchaca Large Igneous Province (LIP) of the Amazonian Craton: Implications for the Rodinia supercontinent. Precambrian Research, 265: 273–285. http://doi.org/10.1016/j.precamres.2014.07.006

Teixeira, W., Reis, N.J., Bettencourt, J.S., Klein, E.L. & Oliveira, D.C. 2019. Intraplate Proterozoic magmatism in the Amazonian Craton reviewed: Geochronology, crustal tectonics and global barcode matches. In: Srivastava, R.K., Ernst, R.E. & Peng, P. (editors), Dyke swarms of the world: A modern perspective. Springer Geology, p. 111–154. Singapore. https://doi.org/10.1007/978-981-13-1666-1_4

Valley, J.W., Lackey, J.S., Cavosie, A.J., Clechenko, C.C., Spicuzza, M.J., Basei, M.A.S., Bindeman, I.N., Ferreira, V.P., Sial, A.N., King, E.M., Peck, W.H., Sinha, A.K. & Wei, C.S. 2005. 4.4 billion years of crustal maturation: Oxygen isotope ratios of magmatic zircon. Contributions to Mineralogy and Petrology, 150: 561–580. https://doi.org/10.1007/s00410-005-0025-8

Vasquez, M., Altenberger, U., Romer, R.L., Sudo, M. & Moreno–Murillo, J.M. 2010. Magmatic evolution of the Andean Eastern Cordillera of Colombia during the Cretaceous: Influence of previous tectonic processes. Journal of South American Earth Sciences, 29(2): 171–186. http://doi.org/10.1016/j.jsames.2009.02.003

Veras, R.da S., Nascimento, R.S.C., Almeida, M.E., Paquette, J.L. & Carneiro, M.C.R. 2018. Paleoproterozoic basement of Içana Domain, Rio Negro Province, northwestern Amazonian Craton: Geology, geochemistry and geochronology (U–Pb and Sm–Nd). Journal of South American Earth Sciences, 86: 384–409. http://doi.org/10.1016/j.jsames.2018.07.003

Vervoort, J.D. & Kemp, A.I.S. 2016. Clarifying the zircon Hf isotope record of crust–mantle evolution. Chemical Geology, 425: 65–75. http://doi.org/10.1016/j.chemgeo.2016.01.023

Vervoort, J.D., Kemp, A.I.S., Fisher, C.M. & Bauer, A.M. 2017. Growth of Earth's earliest crust: The perspective from the depleted mantle. Goldschmidt2017 Conference, Abstracts, 1 p. Paris, France.

Explanation of Acronyms, Abbreviations, and Symbols:

CG	Cuchivero Group
CHUR	Chondritic uniform reservoir
DM	Depleted mantle
GAG	Güejar–Apaporis Graben
GLOOS	Global subducted sediments
ID–TIMS	Isotope dilution thermal ionisation mass spectrometry
IGSN	International Geo Sample Number
KDE	Kernel density estimate
LA–ICP–MS	Laser ablation inductively coupled plasma mass spectrometry
LIPs	Large Igneous Provinces
MI	Mauricio IBAÑEZ–MEJIA
MMC	Mitú Migmatitic Complex
MT	Mud Tank
PP	Putumayo Province
PRORADAM	Proyecto Radargramétrico del Amazonas
REE	Rare earth element
RNJP	Rio Negro–Juruena Province
RSIP	Rondonian–San Ignacio Province
SHRIMP	Sensitive high–resolution ion microprobe
UGC	Umberto G. CORDANI
VSMOW	Vienna standard mean ocean water
VTP	Ventuari–Tapajós Province

Authors' Biographical Notes

Mauricio IBAÑEZ–MEJIA graduated as a geologist from the Universidad Nacional de Colombia, Bogotá, in 2007. He obtained MS (2010) and PhD (2014) degrees in petrology and geochemistry from the University of Arizona, USA, followed by two years as a W.O. Crosby postdoctoral fellow in the Massachusetts Institute of Technology in Cambridge, USA, and four years as an assistant professor in the Department of Earth and Environmental Sciences at University of Rochester, USA. He is currently an assistant professor in the Department of Geosciences at the University of Arizona, USA. His main research interests are in the fields of isotope geochemistry, geochronology, petrology, and crustal evolution.

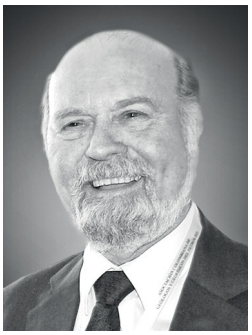

Umberto G. CORDANI graduated in geology in 1960 at the Universidade de São Paulo, Brasil, was hired as Assistant Professor by the same university and obtained his PhD in 1968. In 1980 he completed his teaching career as full professor. Retired, he continues working as Emeritus Professor. His main research interests are in geochronology applied to tectonics and crustal evolution. He had active participation in the international community and was president of the International Union of Geological Sciences (IUGS) from 1988 to 1992. He has received a few honours, including the José Bonifácio Gold Medal of the Brazilian Geological Society, and the Great Cross of Scientific Merit, the highest Brazilian award in science.